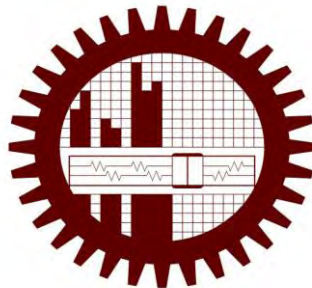# DETECTION OF MECHANICAL DEFORMATION IN OLD AGED POWER TRANSFORMER USING CROSS CORRELATION CO-EFFICIENT ANALYSIS METHOD

A thesis submitted to the Department of Electrical and Electronic Engineering in partial fulfillment of the requirements for the degree of
Master of Science in Electrical and Electronic Engineering (EEE)

By

ASIF ISLAM

Department of Electrical and Electronic Engineering (EEE)
BANGLADESH UNIVERSITY OF ENGINEERING AND YECHNOLOGY (BUET)
DHAKA

May, 2012

Declaration

This is to certify that this work has been done by the undersigned and it has not been submitted elsewhere for the award of any degree or diploma.

Signature of the Student

....
(Asif Islam)

The thesis titled "Detection of Mechanical Deformation in Old Aged Power Transformer Using Cross Correlation Co-Efficient Analysis Method" submitted by Asif Islam, Roll – 0409062127F, Session – April/2009, has been accepted as satisfactory in partial fulfillment of requirements for the degree of Master of Science in Engineering (Electrical and Electronic) on May 19, 2012.

BOARD OF EXAMINERS

1. ………………………………

    (Dr. Aminul Hoque)
    Professor
    Department of EEE, BUET, Dhaka

    Chairman
    (Supervisor)

2. ………………………………

    (Dr. Saifur Rahman)
    Professor and Head
    Department of EEE, BUET, Dhaka

    Member
    (Ex-Officio)

3. ………………………………

    (Dr. Shahidul Islam Khan)
    Professor
    Department of EEE, BUET, Dhaka

    Member

4. ………………………………

    (Dr. Md.Shahid Ullah)
    Professor and Head
    Department of EEE, IUT, Gazipur

    Member
    (External)

ACKNOWLEDGEMENT

ABSTRACT

Detection of minor faults in power transformer active part is essential because minor faults may develop and lead to major faults and finally irretrievable damages occur. Sweep Frequency Response Analysis (SFRA) is an effective low-voltage, off-line diagnostic tool used for finding out any possible winding displacement or mechanical deterioration inside the transformer which happens due to large electromechanical forces occurring from the fault currents or due to transformer transportation and relocation. In this method, the frequency response of a transformer is taken both at manufacturing industry and concern site. Then both the response is compared to predict the fault which has occurred in the active part of transformer. But in old aged transformers, the primary reference response is unavailable. So, Cross Correlation Co-Efficient (CCF) measurement technique can be a new approach for fault detection in these transformers. In this thesis, mathematical analysis of transfer function for SFRA technique has been elaborated, mathematical model for calculating CCF between SFRA curves has been programmed and through several case studies, the developed model has been applied on some faulty transformer. It has been found that theoretically predicted results using CCF matches with practical results which indicate the effectiveness of the newly proposed method. The case studies are based on several 132 kV & 230 kV healthy and faulty power transformers manufactured by Bangladesh, China, India and England.

Contents

List of Figures

List of Tables

List of Principal Abbreviations

SFRA	Sweep Frequency Response Analysis
LVI	Low Voltage Impulse
CCF	Cross Correlation Co-Efficient
IEEE	Institution of Electrical and Electronic Engineers, Inc.
IEC	International Electrotechnical Commission
CEGB	Central Electricity Generation Board
FFT	Fast Fourier Transform
EMF	Electro Magnetic Force
DGA	Dissolved Gas Analysis
BPDB	Bangladesh Power Development Board
DPDC	Dhaka Power Distribution Company Ltd.
PGCB	Power Grid Company of Bangladesh Ltd.
NCF	Normalization Covariance Factor
HV	High Voltage
LV	Low Voltage
UPGD	United Power Generation and Distribution Company Ltd.
EEL	Energypac Engineering Limited

Chapter 1

Introduction

1.1 General Consideration

Nowadays, reliability is an inevitable part of power system studies and operation, due to significant increase in the number of industrial electrical consumers. Power transformer is one of the major and critical elements in power system [1] in the area of reliability issue, since their outage may result in costly and time-consuming repair and replacement. Power transformers are specified to withstand the mechanical forces arising from both shipping and subsequent in-service events, such as faults and lightning. Once a transformer is damaged either heavily or slightly, the ability to withstand further incidents or short circuit test [2] becomes reduced. There is clearly a need to effectively identify such damage. A visual inspection is costly and does not always produce the desired results or conclusion [3]-[5]. During a field inspection, the oil has to be drained and confined space entry rules apply. Often, a complete tear down is required to identify the problem. An alternative method is to implement field-diagnostic techniques that are capable of detecting damage such as Frequency Response Analysis (FRA) [6].

Deregulation of the power distribution industry in recent years has lead to strategies for optimizations of the power networks. As a consequence, the operating stress levels in the networks are closer to the transformers withstand levels [7]-[9] and the amounts of spare capacity in the networks are decreasing. This has lead to increased quality demands on the transformer manufacturers, and an incentive for established transformer assessment routines in the power industry.

In case of Bangladesh power sector, it is mostly a large amount of older equipment that causes increasing interest in efficient assessment methods. Another factor is that new transformers are more optimized and thus more sensitive, which also gives reason for systematical assessment routines [1].

One increasingly important method for transformer condition monitoring is Sweep Frequency Response Analysis (SFRA). SFRA can be used to detect internal damages in a transformer, for

example winding displacements [10]. In operational transformers such damages can be the result of external short-circuits. Other possible causes of damage are incidents during transportation of new or serviced units and aging processes, the latter which for example affect winding insulation. Common to the internal damages that is detectable [11]-[14] by SFRA is their influence on electrical parameters of the transformer windings. For example a displacement of a winding will affect stray capacitances, between wounds and to surrounding structures (tank, core etc.). Such changes are detectable by SFRA and thus possible to detect without dismantling of the transformer [15].

1.2   Review of Literature

Frequency Response measurements were first investigated in depth by Dick and Erven at Ontario Hydro in Canada in the 1970's. For some reason, their work was never accepted widely. In the 1980's the Central Electricity Generating Board (CEGB) in the UK took up the measurement technique and applied it to transmission transformers. The French also began to pursue measurements at the same time. On the break-up of the CEGB in the early 1990's work in Frequency Response Analysis (FRA) was taken up by National Grid in the UK and resulted in several papers at Doble Client Conferences. The technique has been spread further through Euro-Doble conferences and client meetings and several utilities took up the technique.

As the basic technique developed by early users required laboratory based equipment such as HP network analyzers, which were robust, but not field hardened and required specialist operators. Upon a successful program of product development and field trials, Doble stepped in to provide field engineers and staff with a reliable and robust tool for transformer analysis – the M5100. This outperforms the HP in terms of measurement characteristics and field usability.

There are basically two techniques used for FRA measurements on power transformers; Low Voltage Impulse (LVI) based FRA and Sweep Frequency Response Analysis (SFRA) [16]. The two techniques are also termed FRA-I (Impulse method) and FRA-S (Swept-frequency method) [17]. The common strategy for both methods [18] is that the transformer impedance is measured at several different frequencies. The impedance will vary from one frequency to another due to the internal constitution of the transformer.

LVI is based on that a low voltage impulse is injected into a transformer terminal. The impulse comprises the wide range of frequencies that are required and the resulting voltage or, if more suitable, current pulse is measured at other terminals [19]. The response is sampled stored in time domain and transformed to frequency domain using Fast Fourier Transform (FFT).

With SFRA, a frequency sweep of sinusoidal signals is injected to a transformer terminal. For each frequency the injected signal is measured for reference and the response is measured at another terminal of the same winding [20]-[22]. The difference between reference and response is stored in modulus, argument form as magnitude and phase.

Many early practitioners tried impulse systems, and have continued to try them up to the present. Though appealing in terms of speed, they have never been able to match the range, resolution or repeatability of sweep methods and continue to reject impulse methods.

1.3   Objectives of Present Research

This work aims at applying FRA technique for faulty or age-old power transformers in Bangladesh power sectors on site so that if any mechanical deformation is suspected, those will be sent to workshop for repairing. The present work focuses on the following:

1. Developing a transfer function of a power transformer for Sweep Frequency Response Analysis (SFRA) taking all practical constraints e.g. Leakage current, Hysteresis loss, Eddy current loss etc. into account.

2. To overview the existing methods for detection of mechanical displacement in transformers.

3. Implementation of Cross Correlation Co-Efficient (CCF) analysis technique to find out dissimilarity of the response signals got from different phases of a power transformer.

4. Successful prediction of the mechanical displacements or deformations which have taken place in core or coils of a power transformer.

5. Validation of theoretical prediction by fault detection in real damaged transformer using CCF model.

Outcome of the work will be that the prediction about the physical position of the active part of a transformer where the deformation has occurred exactly will be possible.

1.4   Organization of the Thesis

The presentation of the material studied in the present work is organized as follows:

Chapter 1 presents the review of the literature, objectives of the thesis along with the thesis organization.

Chapter 2 discusses the basic principle and construction details of power transformer according with transformer equivalent circuit representation taking all practical loss conditions into account. Causes of different types of transformer faults as well as basic tests for transformer to detect these faults have been elaborated at the last portion of this chapter.

Chapter 3 contains a brief description of Sweep Frequency Response Analysis (SFRA) technique for detection of mechanical deformation in transformer. The response measurement procedure and transfer function analysis for transformer has been described at the first portion of this chapter. Then the standard response from different types of windings has been represented followed by the response analysis bands recommended by IEEE professional experts.

Chapter 4 introduces an effective statistical parameter, Cross Correlation Co-Efficient (CCF) which is used frequently in signal analysis to determine similarity between different traces. The MATLAB code which has been developed in this work to calculate CCF between different SFRA curves, has been described at the last point of this chapter.

Chapter 5 is based on fault detection in power transformers through traditional method using SFRA technique. In this chapter, mechanical deformations in three different power transformers of 230 kV and 132 kV has been detected using experts in view method.

Chapter 6 represents the effectiveness of the proposal to use CCF parameter to detect mechanical faults in power transformer successfully. Through three case studies, CCF has been calculated between different SFRA traces from the power transformers. Depending on the value of CCF, the type and location of the deformation or faults which have taken place in transformer has been predicted. After that, opening the top cover of the transformer, by physical inspection, position and types of deformation has been noted to ensure the effectivity of the new proposal and technique.

Chapter 7 contains the ending discussion as well as scope of future development of this technique.

Chapter 2

Power Transformer and its Internal Faults

2.1   Introduction

Transformer is one of the most vital and important electrical machinery in power transmission and distribution system. The development of the present day power system is very much attributable to the large number and types of transformer that are in operation in the system, such as, generator transformers, step-up transformers [4], step-down transformers, interlinking transformers, power transformers (Figure 2.1) & distribution transformers etc. Being a static machine, it is inherently reliable compared to other machines. Distribution transformers are a important link between the power system and millions of electricity consumers. Any failure of this important equipment, apart from adversely affecting the consumers, will also mean considerable financial loss to the electricity undertaking. It is therefore of important that utmost care is taken in the design, manufacture, testing, installation, and maintenance of transformers.

A transformer consists of a magnetic core made out of insulated silicon steel laminations. Two distinct sets of windings, one called primary and other called secondary winding, are wound on such core. The transformer helps in converting low voltage into high voltage or visa-versa and accordingly the transformer is termed step-up or step-down. The winding to which the voltage is applied is called primary winding, where as the winding to which the load is connected is called secondary winding. The transformer works on the principle of electro-magnetic induction. Such phenomena can take place in a static device, only, if the magnetic flux is continually varying.

Figure 2.1: Power Transformer

It is therefore clear that static transformers can only be used with alternating currents only. When an alternating EMF is applied to the primary winding of a transformer with the secondary winding open circuited, a small current flows in the primary winding which serves to magnetize the core and to feed the iron losses of the transformer. As primary and secondary windings are wound on the same core, the magnetizing flux is the same for both the windings. The magnetizing flux corresponds to the magnetizing current in the primary and the number of turns

of the primary winding [23]. Primary and secondary windings are wound on the same core hence the induced voltage per turn is the same for both primary and secondary winding. Also the absolute value of induced voltage in the primary and secondary windings is proportional to the number of turns in the respective windings [5].

2.2   Construction Details

The main parts of a transformer are:

- Transformer core
- Transformer Windings
- Transformer Tank and Radiators

2.2.1   Transformer Core

Every transformer has a core which is surrounded by windings. The core (Figure 2.2) is made out of special cold rolled grain oriented silicon sheet steel laminations. The special silicon steel ensures low hysteresis losses. The silicon steel laminations also ensure high resistively of core material which results in low eddy currents. In order to reduce eddy current losses, the laminations are kept as thin as possible. The thickness of the laminations is usually around 0.27 to 0.35 mm. The transformer cores construction is of two types, viz, core type and shell type. In core type transformers, the windings are wound around the core, while in shell type transformers, the core is constructed around the windings. The shell type transformers provide a low reactance path for the magnetic flux, while the core type transformer has a high leakage flux and hence higher reactance.

The ideal shape for the section of the core is a circle, as this would mean no wastage of space between the core and windings, except the space taken by the insulation between laminations. A perfectly circular section of core would mean varying dimensions for each successive lamination, which may not be economical. A compromise is therefore struck and a stepped core (four or six steps) construction is normally preferred. The net sectional area is calculated from the dimensions of the various sections and giving due allowance for the insulation thickness. The yoke section is arranged

Figure 2.2: Transformer Core

similar to the limb section. To make the best use of the grain oriented silicon steel it is necessary

that the flux run parallel to the direction of the rolling for as much of the magnetic path as possible [13]. This is achieved by selecting identical cross-section and shape for core and yoke sections and having mitered corners. The materials used are such as to give low hysteretic losses, for a particular flux density. These are dependant on weight of material used and design flux density. In case a low flux density is employed, the weight of material increases, which in turn also leads to increase in length of mean turn of transformer coil. Both these aspects result in increase in losses. Similarly, the eddy current loss depends on the quality of material thickness of laminations and the flux density employed.

The limb laminations in small transformers are held together by stout webbing tape or by suitably spaced glass fiber bends. The use of insulated bolts passing through the limb laminations has been discontinued due to number of instances of core bolt failures. The top and bottom mitered yokes are interleaved with the limbs and are clamped by steel sections held together by insulated yoke bolts. The steel frames clamping the top and bottom yokes are held together by vertical tie bolts.

2.2.2   Transformer Winding

The primary and secondary windings in a core type transformer are of the concentric type only, while in case of shell type transformer these could be of sand-witched type as well. The concentric (Figure 2.3) windings are normally constructed in any of the following types depending on the size and application of the transformer:

- Cross over Type
- Helical Type
- Continuous Disc Type

Cross-over type winding is normally employed where rated currents are up-to about 20 Amperes or so. In this type of winding, each coil consists of number of layers having number of turns per layer. The conductor being a round wire or strip insulated with a paper covering. It is normal practice to provide one or two extra lavers of paper insulation between lavers. Further, the insulation between lavers is wrapped round the end turns of the lavers there by assisting to keep the whole coil compact. The complete winding consists of a number of coils connected in series. The inside end of a coil is connected to the outside end of adjacent coil. Insulation blocks are provided between adjacent coils to ensure free circulation of oil.

In helical winding, the coil consists of a number of rectangular strips wound in parallel racially such that each separate turn occupies the total radial depth of the winding. Each turn is wound on a number of key spacers which form the vertical oil duct and each turn or group of turns is spaced by radial keys sectors. This ensures free circulation of oil in horizontal and vertical direction. This type of coil construction is normally adopted for low voltage windings where the magnitude of current is comparatively large.

The continuous disc type of windings consists of number of Discs wound from a single wire or number of strips in parallel. Each disc consists of number of turns, wound radically, over one another. The conductor passes uninterruptedly from one disc to another. With multiple-strip conductor, Transpositions are made at regular intervals to ensure uniform resistance and length of conductor. The discs are wound on an insulating cylinder spaced from it by strips running the whole length of the cylinder and separated from one another by hard pressboard sectors keyed to the vertical strips. This ensures free circulation of oil in horizontal and vertical direction and provides efficient heat dissipation from windings to the oil. The whole coil structure is mechanically sound and capable of resisting the most enormous short circuit forces.

Figure 2.3: Transformer Coil

The insulation of the windings comprises of insulating cylinders between LV windings and core and between HV winding (Figure 2.4). Also insulating barriers are provided where necessary between adjacent limbs, in some cases and between core yoke and coils. The leads from top and bottom end of windings and from such tapings, as may be provided are brought out to a few centimeters length only. The electrical connection from these leads to the terminals or

Figure 2.4: Insulation of Transformer

bushings consist of either copper rod or strips depending on the current to be carried. Copper rods are insulated with Bakelite tubes and supported by cleats. Which in turn, are supported from the vertical tie rods passing through the top and bottom yoke clamp. When copper strips are used for low voltage leads no insulation need to be provided, except the cleats, which hold the strip in position. The strips are however wrapped with linen or varnish cloth at the point where it passes through the leads. Leads from tapings are brought out (Figure 2.5) to a point just below the top oil and so arranged that tapings may be readily changed by means of off-load Tap changer.

Figure 2.5: Core-Coil assembled active part

2.2.3   Transformer Tank

Transformer tanks commonly used are of the following types:

- Plain sheet steel tank
- Sheet steel tank with external cooling tubes
- Radiator tanks
- Tanks with corrugated wall panels

Plain sheet steel tanks (Figure 2.6) are used where the size of the tank provides adequate cooling surface to dissipate the heat generated on account of losses inside the transformer. Normally transformers up-to 50KVA could be manufactured without external cooling tubes. For transformers of higher rating, tanks are constructed with external cooling tubes to provide additional surface for heat dissipation. The cooling tubes could be circular or elliptical. Elliptical tubes with smaller width are employed where one of the sides of the transformer is fully occupied by on load tap changer. This ensures more tubes on the given surface thereby providing more area for heat dissipation. In larger tanks, stiffeners are also provided on the sides of the tank to prevent bulging of the tank under oil pressure. The tubes are welded on the inside of the tank, while all other joints are welded both, inside and outside.

Large size transformers, above 5 MVA rating are normally provided with detachable Radiator banks to provide required cooling surface. The radiator bank consists of series of elliptical tubes or a pressed steel plate assembly welded into top and bottom headers. The radiator bank is bolted on to the tank wall and two isolating valves are fitted into the oil inlet and outlet. In case of very large transformers, even detachable radiator banks mounted onto the tank walls do not provide adequate cooling surface. In such cases, separate self supporting coolers are provided which are

Figure 2.6: Transformer Tank

connected to the main transformer through large detachable pipes. This type of arrangement is good for naturally cooled transformers, as well as, for forced cooled transformers. Forced air cooling could be provided by means of suitable fans located below the cooler banks. Similarly, forced oil cooling could be provided by installing an oil pump in the return cold oil pipe connecting the main transformer tank to the cooler bank. For outdoor transformers, the transformer has to be water-tight. For this purpose, the cover bolts are closely spaced and a substantial tank flange of ample width is provided. Further a Neoprene bonded cork gasket is provided between the tank flange and the cover. The bushing insulators are selected considering the maximum system voltages encountered in the system and pollution conditions prevailing at site. The joints are made water-tight by use of Neoprene bonded cork gaskets.

2.3 Basic Principle

The transformer is based on two principles: firstly, that an electric current can produce a magnetic field (electromagnetism) and secondly that a changing magnetic field within a coil of wire induces a voltage across the ends of the coil (electromagnetic induction). By changing the current in the primary coil, it changes the strength of its magnetic field; since the changing magnetic field extends into the secondary coil, a voltage is induced across the secondary.

A simplified transformer design is shown in Figure 2.7. A current passing through the primary coil creates a magnetic field. The primary and secondary coils are wrapped around a core of very high magnetic permeability, such as iron; this ensures that most of the magnetic field lines produced by the primary current are within the iron and pass through the secondary coil as well as the primary coil.
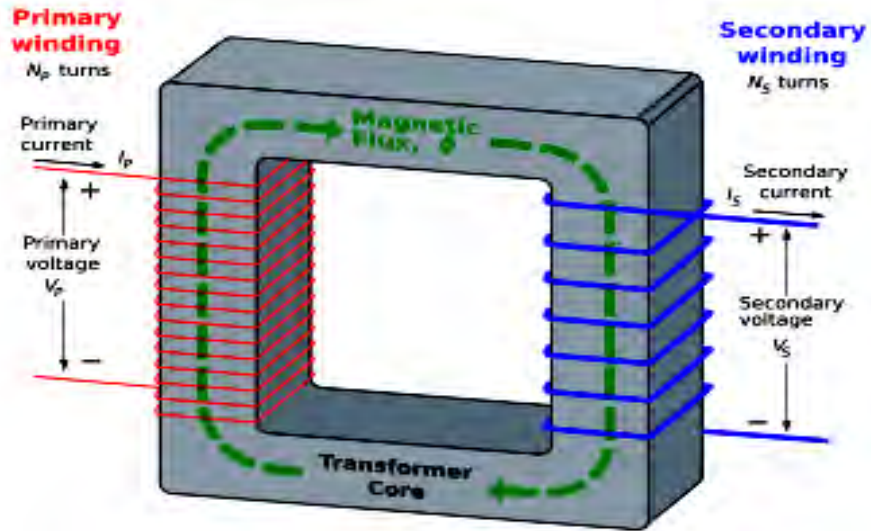
Figure 2.7: An ideal step-down transformer showing magnetic flux in the core

The voltage induced across the secondary coil may be calculated from Faraday's law of induction, which states that:

$$V_S = N_S \frac{d\varphi}{dt}$$

where V_S is the instantaneous voltage, N_S is the number of turns in the secondary coil and Φ equals the magnetic flux through one turn of the coil. If the turns of the coil are oriented perpendicular to the magnetic field lines, the flux is the product of the magnetic field strength B and the area A through which it cuts. The area is constant, being equal to the cross-sectional area of the transformer core, whereas the magnetic field varies with time according to the excitation of the primary. Since the same magnetic flux passes through both the primary and secondary coils in an ideal transformer, the instantaneous voltage across the primary winding equals

$$V_P = N_P \frac{d\varphi}{dt}$$

Taking the ratio of the two equations for V_S and V_P gives the basic equation for stepping up or stepping down the voltage

$$\frac{V_P}{V_S} = \frac{N_P}{N_S}$$

If the secondary coil is attached to a load that allows current to flow, electrical power is transmitted from the primary circuit to the secondary circuit. Ideally, the transformer is perfectly efficient; all the incoming energy is transformed from the primary circuit to the magnetic field

and into the secondary circuit. If this condition is met, the incoming electric power must equal the outgoing power.

$$P_{incoming} = I_P V_P = P_{outgoing} = I_S V_S$$

giving the ideal transformer equation

$$\frac{V_P}{V_S} = \frac{N_P}{N_S} = \frac{I_S}{I_P}$$

If the voltage is increased (stepped up) ($V_S > V_P$), then the current is decreased (stepped down) ($I_S < I_P$) by the same factor. Transformers are efficient so this formula is a reasonable approximation.
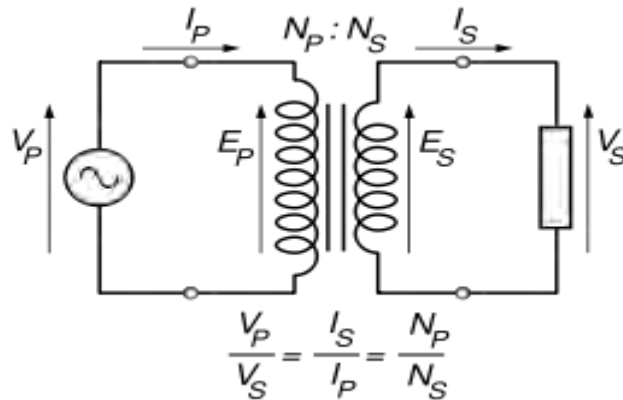
Figure 2.8: The ideal transformer as a circuit element

The model of an ideal transformer typically assumes a core of negligible reluctance with two windings of zero resistance. When a voltage is applied to the primary winding, a small current flows, driving flux around the magnetic circuit of the core. The current required to create the flux is termed the *magnetizing current*; since the ideal core has been assumed to have near-zero reluctance, the magnetizing current is negligible, although still required to create the magnetic field. The simplified description above neglects several practical factors, in particular the primary current required to establish a magnetic field in the core, and the contribution to the field due to current in the secondary circuit.

2.4   Practical Considerations

2.4.1   Leakage Flux

The ideal transformer model assumes that all flux generated by the primary winding links all the turns of every winding, including itself. In practice, some flux traverses paths that take it outside the windings. Such flux is termed *leakage flux*, and results in leakage inductance in series with the mutually coupled transformer windings. Leakage results in energy being alternately stored in and discharged from the magnetic fields with each cycle of the power supply. It is not directly a power loss, but results in inferior voltage regulation, causing the secondary voltage to fail to be directly proportional to the primary, particularly under heavy load. Transformers are therefore normally designed to have very low leakage inductance.
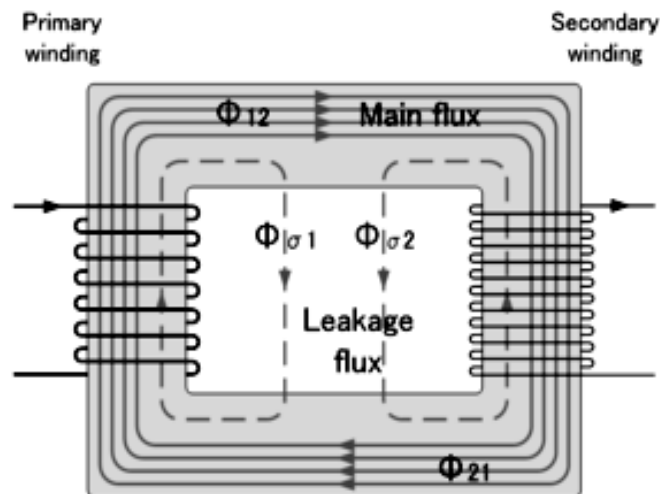
Figure 2.9: Leakage flux of a transformer

However, in some applications, leakage can be a desirable property, and long magnetic paths, air gaps, or magnetic bypass shunts may be deliberately introduced to a transformer's design to limit the short-circuit current it will supply. Leaky transformers may be used to supply loads that exhibit negative resistance, such as electric arcs, mercury vapor lamps, and neon signs; or for safely handling loads that become periodically short-circuited such as electric arc welders. Air gaps are also used to keep a transformer from saturating, especially audio-frequency transformers in circuits that have a direct current flowing through the windings.

2.4.2 Energy Losses

An ideal transformer would have no energy losses and would be 100% efficient. In practical transformers energy is dissipated in the windings, core, and surrounding structures. Larger transformers are generally more efficient, and those rated for electricity distribution usually perform better than 98%. Experimental transformers using superconducting windings have achieved efficiencies of 99.85%. While the increase in efficiency is small, when applied to large heavily-loaded transformers the annual savings in energy losses is significant.

A small transformer, such as a plug-in "wall-wart" or power adapter type used for low-power consumer electronics, may be no more than 85% efficient, with considerable loss even when not supplying any load. Though individual power loss is small, the aggregate losses from the very large number of such devices are coming under increased scrutiny. The losses vary with load current, and may be expressed as "no-load" or "full-load" loss. Winding resistance dominates load losses, whereas hysteresis and eddy currents losses contribute to over 99% of the no-load loss. The no-load loss can be significant, meaning that even an idle transformer constitutes a drain on an electrical supply, which encourages development of low-loss transformers.

Transformer losses are divided into losses in the windings, termed copper loss, and those in the magnetic circuit, termed iron loss. Losses in the transformer arise from:

- **Winding resistance**

  Current flowing through the windings causes resistive heating of the conductors. At higher frequencies, skin effect and proximity effect create additional winding resistance and losses.

- **Hysteresis losses**

  Each time the magnetic field is reversed, a small amount of energy is lost due to hysteresis within the core. For a given core material, the loss is proportional to the frequency and is a function of the peak flux density to which it is subjected.

- **Eddy currents**

  Ferromagnetic materials are also good conductors, and a solid core made from such a material also constitutes a single short-circuited turn throughout its entire length. Eddy currents therefore circulate within the core in a plane normal to the flux, and are responsible for resistive heating of the core material. The eddy current loss is a complex function of the square of supply frequency and Inverse Square of the material thickness.

- **Magnetostriction**

  Magnetic flux in a ferromagnetic material, such as the core, causes it to physically expand and contract slightly with each cycle of the magnetic field, an effect known as magnetostriction. This produces the buzzing sound commonly associated with transformers and in turn causes losses due to frictional heating in susceptible cores.

- **Mechanical losses**

  In addition to magnetostriction, the alternating magnetic field causes fluctuating electromagnetic forces between the primary and secondary windings. These incite vibrations within nearby metalwork, adding to the buzzing noise, and consuming a small amount of power.

- **Stray losses**

  Leakage inductance is by itself lossless, since energy supplied to its magnetic fields is returned to the supply with the next half-cycle. However, any leakage flux that intercepts nearby conductive materials such as the transformer's support structure will give rise to Eddy currents and be converted to heat.

2.5   Equivalent Circuit

The physical limitations of the practical transformer may be brought together as an equivalent circuit model (shown below) built around an ideal lossless transformer. Power loss in the windings is current-dependent and is represented as in-series resistances R_P and R_S. Flux leakage results in a fraction of the applied voltage dropped without contributing to the mutual coupling, and thus can be modeled as reactance of each leakage inductance X_P and X_S in series with the perfectly-coupled region.

Iron losses are caused mostly by hysteresis and eddy current effects in the core, and are proportional to the square of the core flux for operation at a given frequency. Since the core flux is proportional to the applied voltage, the iron loss can be represented by a resistance R_C in parallel with the ideal transformer. A core with finite permeability requires a magnetizing current I_M to maintain the mutual flux in the core. The magnetizing current is in phase with the flux; saturation effects cause the relationship between the two to be non-linear, but for simplicity this effect tends to be ignored in most circuit equivalents. With a sinusoidal supply, the core flux lags the induced EMF by 90° and this effect can be modeled as a magnetizing reactance (reactance of

an effective inductance) X_M in parallel with the core loss component. R_C and X_M are sometimes together termed the *magnetizing branch* of the model. If the secondary winding is made open-circuit, the current I_0 taken by the magnetizing branch represents the transformer's no-load current.

The secondary impedance R_S and X_S is frequently moved (or "referred") to the primary side after multiplying the components by the impedance scaling factor $(\dfrac{N_P}{N_S})^2$.
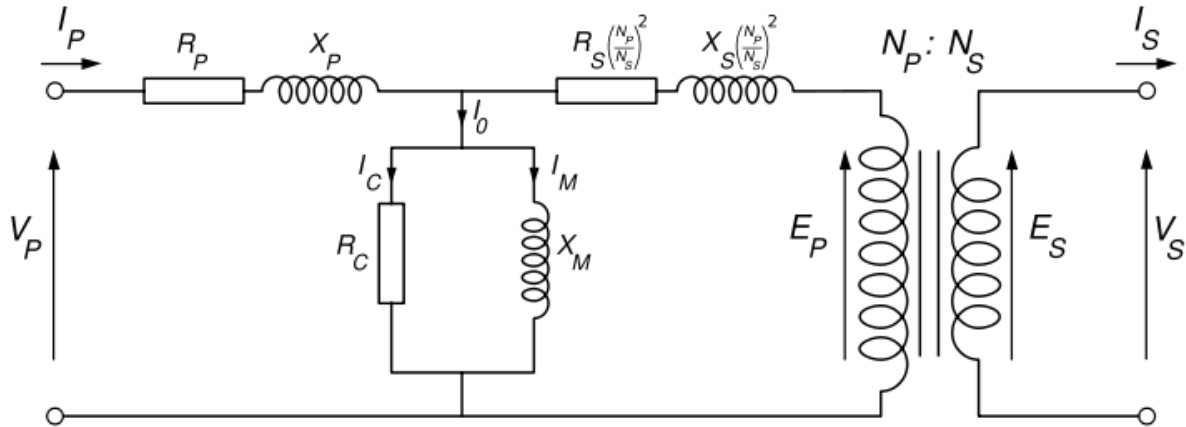
Figure 2.10: Transformer equivalent circuit, with secondary impedances referred to the primary side

The resulting model is sometimes termed the "exact equivalent circuit", though it retains a number of approximations, such as an assumption of linearity. Analysis may be simplified by moving the magnetizing branch to the left of the primary impedance, an implicit assumption that the magnetizing current is low, and then summing primary and referred secondary impedances, resulting in so-called equivalent impedance.

In practical situation, due to voltage difference between Primary and Secondary winding; Primary winding turns and grounded tank body; Secondary winding turns and grounded tank body; different turns of Primary and Secondary windings, capacitance develop between them. This scenario can be represented by the equivalent circuit shown in figure 2.11 where Cgp, Cgs, Cp, Cs and Cw corresponds to Capacitance between Primary winding turns and grounded tank body, Capacitance between Secondary winding turns and grounded tank body, Capacitance between the turns of Primary winding, Capacitance between the turns of Secondary winding and Capacitance between Primary & Secondary windings.
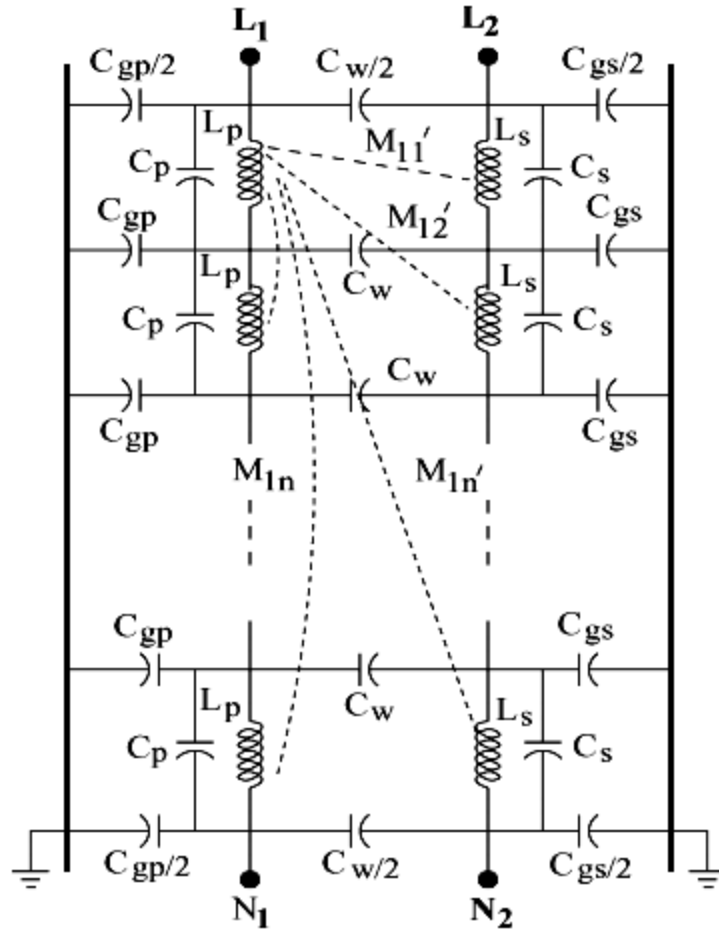
Figure 2.11: Equivalent-circuit representation of a two-winding transformer

2.6 Causes of Internal Faults in Transformer

2.6.1 External Short-Circuit

An external short-circuit of a transformer often results in severe damages on transformer windings. The generating capacity in power distribution networks has increased over the years, due to demands on more electrical power. This has lead to high short circuit capacity in modern transmission networks, which implies increased stress on a transformer in event of an external short circuit. Failure rate in case of a short circuit is 40% for transformers above 100 MVA rating.

A short-circuit causes unidirectional pulsating forces that are proportional to the square of the short-circuit current. This leads to severe stress on the windings and might cause damages.

Repeated inrush currents, especially due to frequent switching on the inner winding, are also known to cause stresses that can lead to failure.

Examples of fault conditions:

- o Deformed, loosened, displaced or collapsed winding structure
- o Buckled hoops
- o Loosened clamping structure
- o Turn-to-turn fault caused by shifted windings (one winding passing over another due to compressing forces)

2.6.2 Over-Voltage Surges

Lightning strikes and switching operations might cause very fast transient overvoltage, especially when the input surge is equal to some of the transformers internal resonance frequencies. This phenomenon is known to cause flashover from turn to core and between turns. Especially turn to turn insulation is sensitive. Insulation damages can lead to Turn-to-turn fault. In severe cases several turns might be welded in various combinations, resulting in lost turns.

2.6.3 Transportation

Incidents during transport of new or serviced transformers can cause damages to it's internal structure. Even if a minor damage occurs, such as a slight looseness in part of a winding, it can lead to breakdown of the transformer e.g. at a future short-circuit current.

2.6.4 Seismic Events

Seismic events such as earthquakes can cause mechanical stress on transformers and cause internal damages.

2.7 Transformer Tests before Commissioning

2.7.1 Ratio, Polarity and Phase relationship test

The ratio should be checked at all taps and between all the windings. Ratio is usually checked by applying a single phase 230V (Approx) supply on the high voltage side and measuring the

voltage on the low voltage side at all tap positions. The measured voltage on LV side shall conform to declining trend between tap (min) to tap (max) position for all phases.

Polarity and interphone connections are checked while measuring the ratio. This can be checked by the Avometer method. The primary and secondary windings are connected together at points indicated in sketch shown below. A low voltage three phase supply is then applied to the HV terminals. Voltage measurements are then taken between various pairs of terminals as indicated in the diagram. Readings obtained should be the vector sum of the separate voltages of each winding under consideration.

2.7.2 Insulation Resistance test

The insulation resistance between winding and earth should be measured with a good 2500/1000 Volts Megger and values should be compared to the test report values. It is preferable to have a motor operated Megger and the readings taken after one minute from starting. Before measuring the insulation resistance, it should be made sure that the bushings are cleaned thoroughly with clean cotton cloth. The lead wires of the Meaggers should not have joints. They should also give reading of more than maximum value readable on the Megger.

2.7.3 Magnetizing Current test

A three phase 415 Volts supply is given to the HV winding of the three phase transformer and simultaneous current readings of the three phases are taken using low range AC ammeters of the same accuracy class. Values should be recorded for the future reference.

2.7.4 Magnetic Balance test

A single phase supply of approximately 230 Volts is applied to one phase of HV winding and the induced voltage on other two HV phases measured separately. Test voltage should be applied to HV winding only. Applying voltage LV winding may induce abnormal high voltage in HV winding which may prove hazardous. Tests should be carried out on all three phases.

When single phase supply is given to middle phase the   induced voltage measured on two extreme phases should be approximately equal. If supply is given to one extreme phase induced voltage on middle phase is expected to be substantially high than the other extreme phase. In each test the sum of the induced voltages on other two phases would be within +/-5% of the applied voltage. 230 Volts single phase supply be given between lines, if windings are delta

connected and induced voltages measured between the other two phases. Whereas supply is given to line and neutral of one phase in case of star connected windings, induced voltages should be measured between the line and neutral of other two phases.

2.7.5 Oil Sample test

Oil after filtration should meet the requirements as laid down under the clause specification. However, to know the conditions the following preliminary tests can be carried out. When tested in accordance with IEC – 600296 and IS 6792 electric strength (Break down voltage should not be less than 50 KVA RMS) test should be carried out six times on the same sample and the result obtained will be arithmetic means of six result.

2.8 Conclusion

In this chapter, basic construction, equivalent circuit as well as basic testing procedures for power transformer have been discussed. The information was based on IEC (International Electrotechnical Commission) – 60067 which was first published in 1987 and it's extended versions.

Chapter 3

Sweep Frequency Response Analysis

3.1   Measurement Procedure

The SFRA "Generator" (Gen.) generates a sinusoidal voltage at a selected frequency and measures the input voltages, amplitude and phase, on two input channels "Reference" (Ref.) and "Measure" (Meas.). The instrument stores "Amplitude" and "Phase" data for both "Reference" channel and "Measure" channel as well as the ratio "Measure" divided by "Reference".
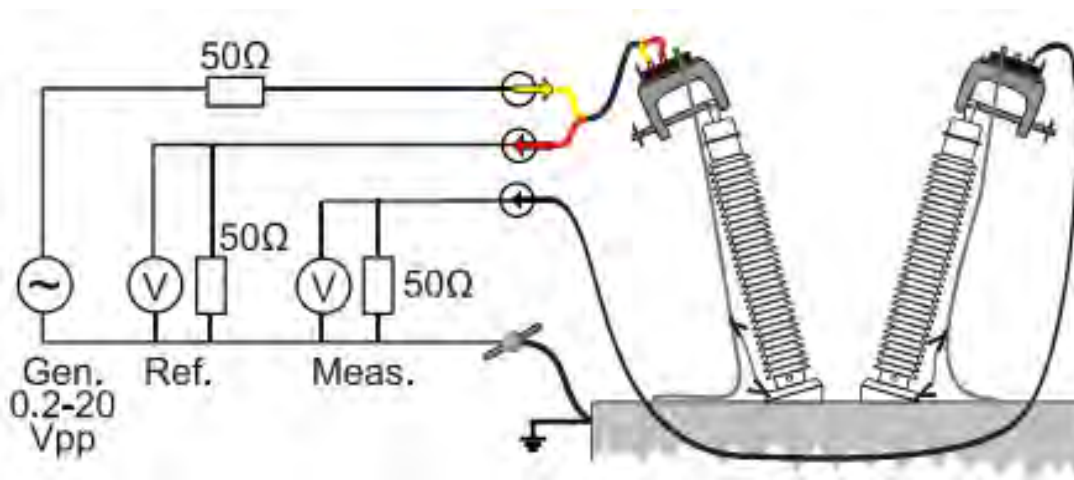
Figure 3.1: SFRA Terminal Connection

SFRA is based on analysis of a winding's transfer function. The signal generator (Figure-3.1) produces a sweep of signals (sine waves) with increasing frequency. The reference and response voltages are logged and processed so that a response curve can be plotted. The response curve shows the relationship between the two voltages (attenuation) as a function of the frequency. The phase shift between reference and response are also measured and can be plotted as a function of frequency.

3.2   Input and Response

With the SFRA method input and output signals are measured at one frequency a time, within a frequency range [24]. How the input signal (x) is affected by the specimen's characteristics will depend upon, what is mathematically described as, the transfer function $H(s) = \dfrac{Y(s)}{X(s)}$ (where s is a frequency dependant parameter, which for continuous sinusoids equals to $j\omega$) (Figure – 3.2).
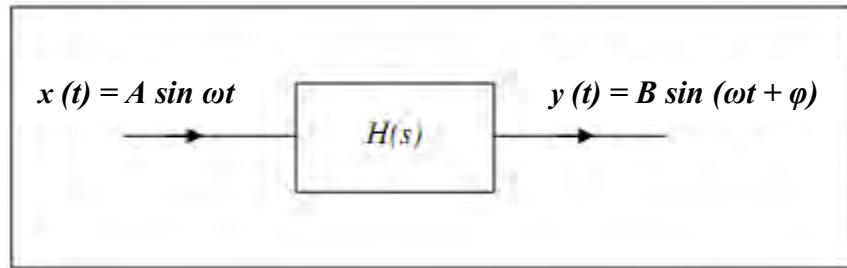
Figure 3.2: Linear Transfer Function with sine wave input

The transfer function is physically the combination of inductance, capacitance and resistance within the specimen (i.e. the admittance or, if inverted, the impedance). When the sinusoidal input signal is applied there will be a dynamic response, dependant on the transfer function. After a while (duration depending on the transfer function) the signal will stabilize into a steady state. Now the response will (ideally) be a sine wave (y), but the amplitude and phase might be different from the input sine wave. Again the transfer function will affect how the response will differ from the input.
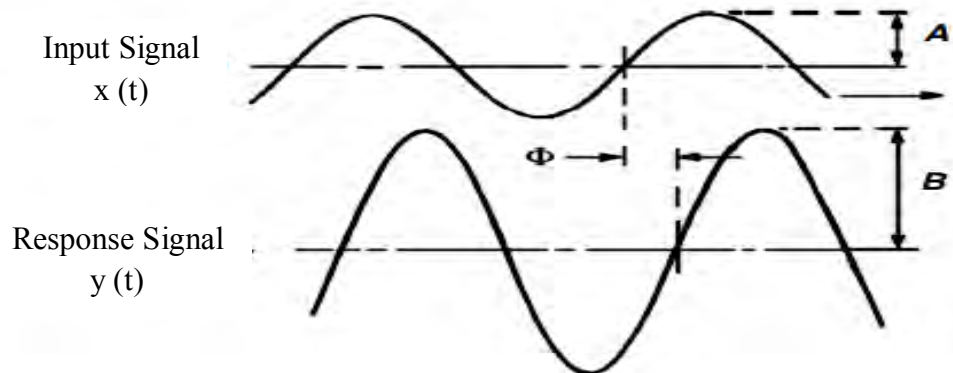
Figure 3.3: Sinusoidal input and steady-state response as displayed on an oscilloscope

The difference in amplitude and phase can be measured with an oscilloscope as shown in Figure-3.3. The normal case when measuring a transformer will be that the response is attenuated (B<A), since there are no active components in the specimen (no gain).
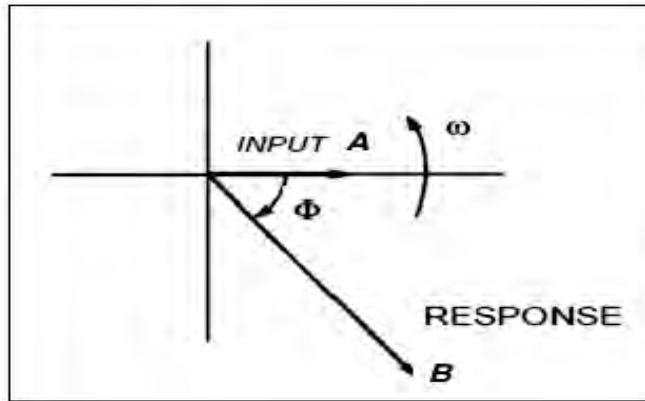
Figure 3.4: Input-Response in vector form (Modulus-Argument)

The signals can also be represented by vectors in the complex plane as in Figure 3.4.
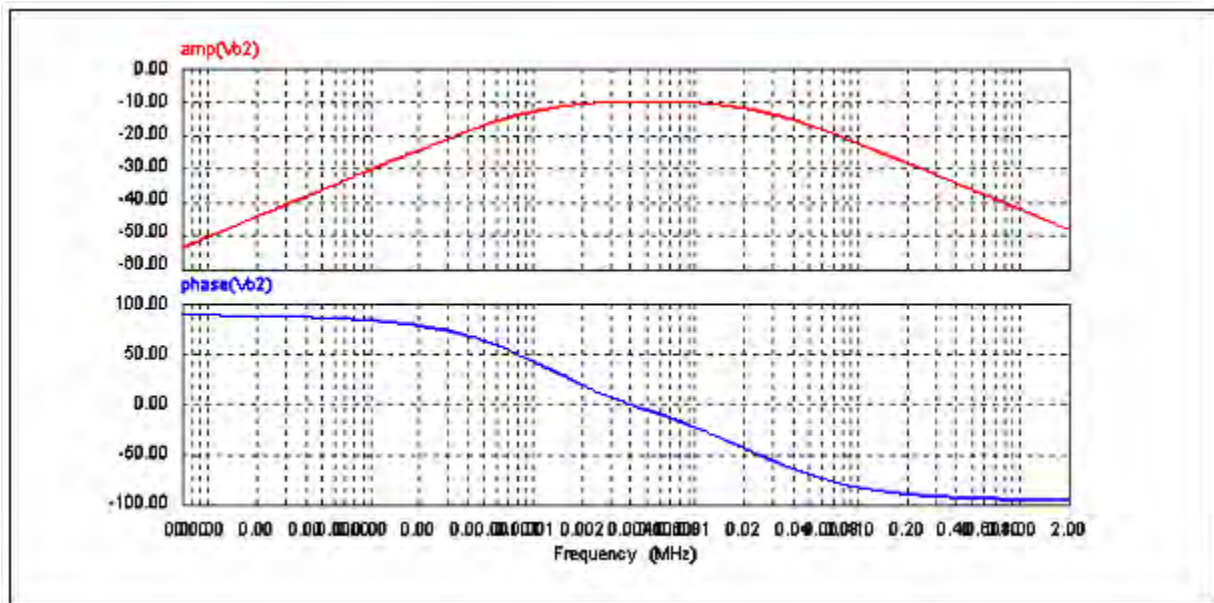
Figure 3.5: Bode plot of an RLC circuit (PSIM [14])

When a range of frequencies have been measured, a plot of attenuation and phase can be made. A so called Bode plot (Figure - 3.5) consists of two separate diagrams, attenuation/frequency and phase/frequency. So, from exact measurements at each frequency, over a range of frequencies, characteristic response curves can be plotted. The response curves can be used for analysis of the transfer function for a specific specimen.

3.3   Two Port Network

When a transformer is subjected to FRA testing, the leads are configured in such a manner that four terminals are used. These four terminals can be divided into two unique pairs [6], [8], [19], one pair for the input and the other pair for the output. These terminals can be modeled in a two-terminal pair or a two-port network configuration. Figure 3.6 illustrates a two-port network where z_{11}, z_{22}, z_{12} and z_{21} are the open-circuit impedance parameters.
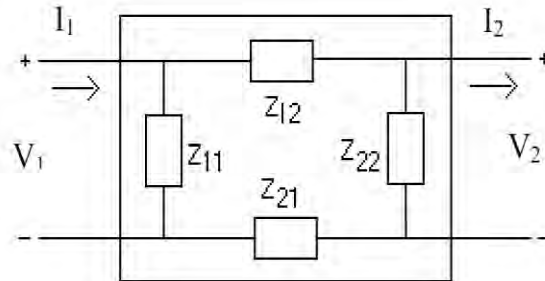
Figure 3.6: Two port network

z_{11}, z_{22}, z_{12} and z_{21} determined by setting each current to zero and solving the following equation

$$\begin{bmatrix} V_1 \\ V_2 \end{bmatrix} = \begin{bmatrix} z_{11} & z_{12} \\ z_{21} & z_{22} \end{bmatrix} \begin{bmatrix} I_1 \\ I_2 \end{bmatrix} \text{ ,where}$$

$$z_{11} = \frac{V_1}{I_1}\bigg|_{I_2=0} \Rightarrow z_{12} = \frac{V_1}{I_2}\bigg|_{I_1=0} \Rightarrow z_{21} = \frac{V_2}{I_1}\bigg|_{I_2=0} \Rightarrow z_{22} = \frac{V_2}{I_2}\bigg|_{I_1=0}$$

These impedances are formed by the complex RLC network of the specimen. The transfer function of this network [20] is represented in the frequency domain and is denoted by the Fourier variable $H(j\omega)$, where $(j\omega)$ denotes the presence of a frequency dependent function and $\omega = 2\pi f$. The Fourier relationship for the input/output transfer function is given by Equation 3.1

$$H(j\omega) = \frac{V_{output}(j\omega)}{V_{input}(j\omega)} \quad \dots \quad \dots \quad \dots (3.1)$$

When a transfer function is reduced to its simplest form, it generates a ratio of two polynomials. The main characteristics, such as half-power and resonance of a transfer function occur at the roots of the polynomials. The roots of the numerator are referred to as ―zeros‖ and the roots of the denominator are ―poles‖ [21]. Zeros produce an increase in gain while poles cause attenuation.

3.4   Transfer Function Analysis

The goal of FRA is to measure the impedance model [25] of the test specimen. When the transfer function H(jω) is measured, it does not isolate the true specimen impedance Z(jω). The true specimen impedance Z(jω) is the RLC network which is positioned between the instrument leads and it does not include any impedance supplied by the test instrument. Figure 3.7 illustrates the RLC circuit with shunt resistor.
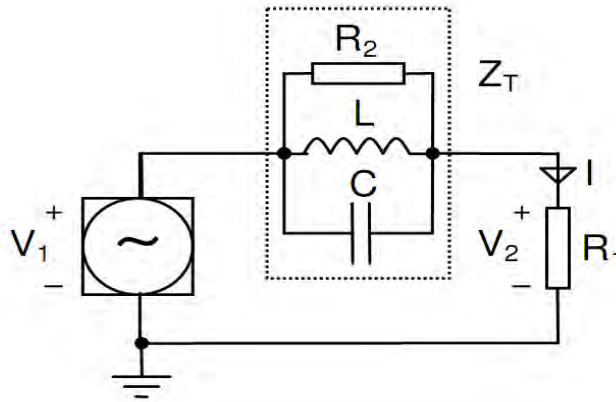
Figure 3.7: RLC circuit and shunt resistor

From the figure, Voltage division formula gives

$$V_2(j\omega) = V_1(j\omega) . \frac{R1}{R1 + \cfrac{1}{\frac{1}{R2} + \frac{1}{j\omega L} + j\omega C}}$$

The transfer function is:

$$H(j\omega) = \frac{V_2(j\omega)}{V_1(j\omega)} = \frac{R_1}{R_1 + \cfrac{1}{\frac{1}{R_2} + \frac{1}{j\omega L} + j\omega C}}$$

$$= \frac{R_1 \left(\frac{1}{R_2} + \frac{1}{j\omega L} + j\omega C\right)}{R_1 \left(\frac{1}{R_2} + \frac{1}{j\omega L} + j\omega C\right) + 1} \cdot \frac{j\omega L}{j\omega L}$$

$$= \frac{R_1 \left(j\omega \frac{L}{R_2} + 1 - \omega^2 LC\right)}{R_1 \left(j\omega \frac{L}{R_2} + 1 - \omega^2 LC\right) + j\omega L}$$

If R_2 would be removed from the circuit then the term $j\omega \frac{L}{R_2}$ disappears from the expressions above. It is now easy to see where the resonant frequency must occur: $1 - \omega_r^2 LC = 0 \Rightarrow \omega_r = \frac{1}{\sqrt{LC}}$

At resonant frequency the transfer function is

$$H\,(j\omega_r) = \frac{R_1(j\frac{L}{R_2\sqrt{LC}} + 1 - 1)}{R_1(j\frac{L}{R_2\sqrt{LC}} + 1 - 1) + j\frac{L}{\sqrt{LC}}}$$

$$= \frac{\frac{R_1}{R_2}}{\frac{R_1}{R_2} + 1}$$

$$= \frac{R_1}{R_1 + R_2}$$

What is really measured over the shunt resistor R_1 is the current I. So, the transfer function describes the admittance: $Y = \frac{I}{V_1}$. The impedance is thus: $Z = \frac{V_1}{I}$

The impedance at resonance (including the shunt resistor) is $Z(\omega_r) = \frac{R_1 + R_2}{R_1}$ … … … (3.2)

The preferred method of engineers is to use the Bode Diagram. The Bode Diagram plots the magnitude and phase as follows:

$$A(dB) = 20log_{10}(H(j\omega)) \qquad … \quad … \quad … \ (3.3)$$

$$A(\Theta) = tan^{-1}(H(j\omega)) \qquad … \quad … \quad … \ (3.4)$$

The Bode Diagram [22] takes advantage of the asymptotic symmetry by using a logarithmic scale for frequency. It is more advantageous to plot H(s) logarithmically over large frequency spans. The logarithmic plot helps to maintain consistent resolution. Plots ranging from 10 Hz to 10 MHz can be displayed as a single plot if they are formatted logarithmically.

3.5   Response of Different Winding Type

Most people immediately think of winding measurements as being only associated with the high-voltage and the low-voltage windings. When considering SFRA measurements, winding measurements realistically consist of five categories and not just two. The winding categories are high-voltage, low-voltage, inter, series, and common.

Short circuit measurements made on one winding while short circuiting another winding are a variation on inter-winding measurements. It should be noted that inter-winding measurement is not a true winding measurement, but rather the transfer impedance between two windings. The series and common winding measurements describe the SFRA application as it is applied to auto transformers. Regardless, certain expectations can be made for each. These measurement types produce some predictable characteristics and properties. Understanding these properties minimize testing error and help to identify problems. The following expectations exist for each of the following categories.

3.5.1   High-Voltage Winding

High-voltage winding measurements have greatest attenuation as compared to low voltage and tertiary windings. Most traces start between –30 dB and –50 dB and are initially inductive. High-voltage windings are much larger in overall size, which contributes to greater complexity in its distributive network. High-voltage winding measurements generally produce steeper resonances and more of them as compared to its low-voltage counterpart. Figure 3.8 illustrates this feature.
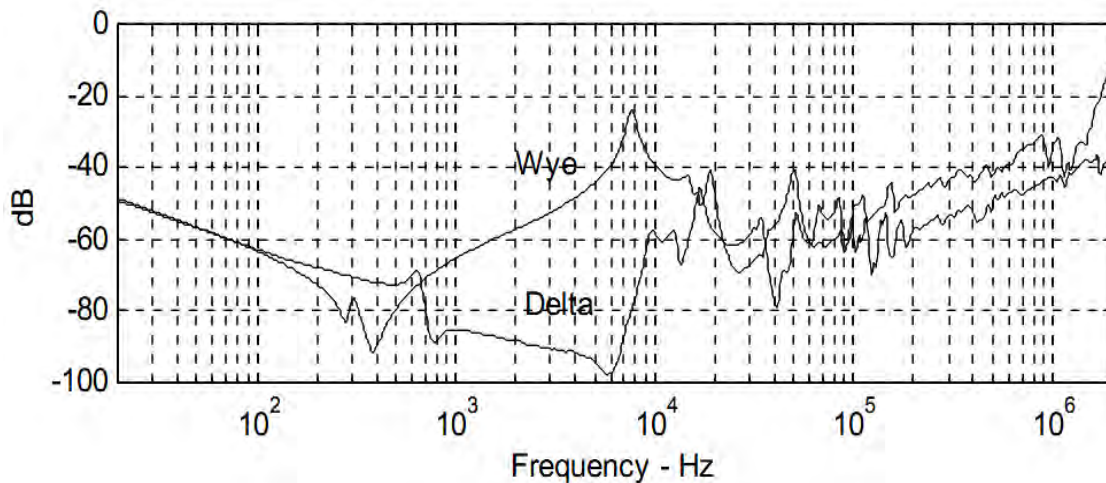
Figure 3.8: High-Voltage Winding response

The traces shown in Figure 3.8 are from different test specimens. Both traces are from 230 kV core-form transformers, however one trace is from a delta connected configuration and the other is from a wye connected configuration.

3.5.2 Low-Voltage Winding

Low-voltage winding measurements have least attenuation as compared to the other categories. Most traces start between –5 dB and –15 dB and are also initially inductive. This characteristic is due to the low impedance property of the high current side of the transformer. The first peak after the core resonance generally approaches –5 dB to 0 dB and is concave and smooth. As compared to the high-voltage winding response, the low-voltage winding fewer fluctuations and is slight smoother. Figure 3.9 illustrates these features. Again, both traces in this figure are from different transformers.
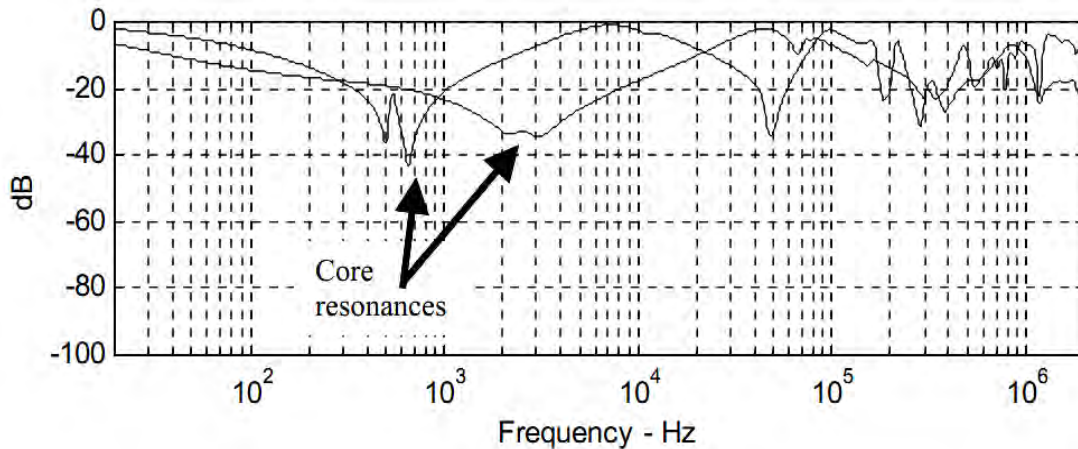
Figure 3.9: Low-Voltage Winding response

3.5.3 Inter Winding

Inter-winding measurements always start with high attenuation, between –60 dB and –90 dB, and are capacitive. If electrostatic interference is present, it will show up at 60 Hz and at the associated harmonics of 60 Hz during this measurement. Figure 3.10 illustrates these features. These traces are very common; most inter-winding traces adhere to one of the basic shapes shown below.
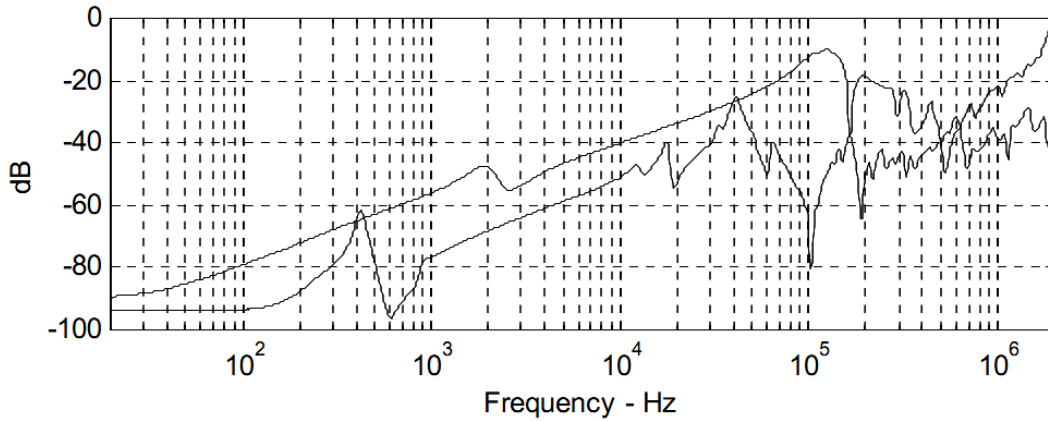
Figure 3.10: Inter Winding response

3.5.4 Complete Response

Figure 3.11 presents a high-voltage winding trace, a low-voltage winding trace, and an inter-winding trace together from a common test specimen. This illustrates their general relationship. It can be seen that the low-voltage winding has consistently lower attenuation then the high-voltage winding. Also, low-voltage winding is much smoother at higher frequencies. This example was taken from a 10 MVA auxiliary transformer.
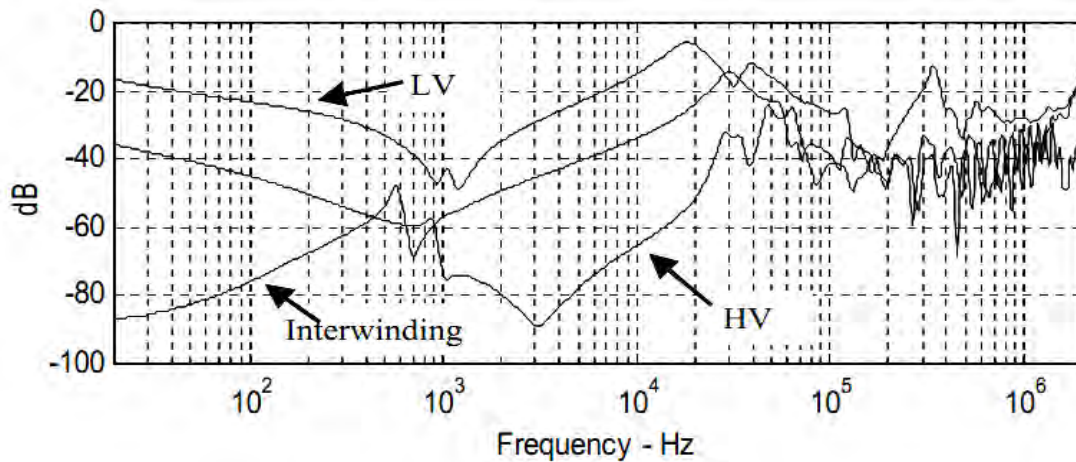
Figure 3.11: Complete Trace response

3.6   Response Analysis Bands

The interpretation of SFRA response takes some experience, but there are guidelines available and some general conclusions can be made from known results.

It is useful to divide the frequency ranges to improve the analysis. The following definitions are taken from a paper published at Cigré Session 2004 [10]:

- Frequency <10 kHz: in this range phenomena linked with the transformer core and magnetic circuits are found. The analysis in this range must take into consideration the residual magnetization which can slightly modify the obtained response from one test to the other. Detectable problems in this range are: coil faults, winding interruptions and magnetic circuit problems.

- Frequency in the range 5 kHz to 500 kHz: in this range phenomena linked with radial relative geometrical movements between windings are detected.

- Frequency > 200 kHz: in this range axial deformations of each single winding are detectable.

For comparison a section from a document titled ―Facilities Instructions, Standards and Techniques" from United States Department of Interior, Bureau of Reclamation [17].

―By comparing future traces with baseline traces, the following can be noted. In general, the traces will change shape and be distorted in the low frequency range (under 5,000 Hz) if there is a core problem. The traces will be distorted and change shape in higher frequencies (above 10,000 Hz) if there is a winding problem. Changes of less than 3 decibels (dB) compared to baseline traces are normal and within tolerances. From 5 Hz to 2 kilohertz (kHz), changes of + or − 3 dB (or more) can indicate shorted turns, open circuit, residual magnetism, or core movement. From 50 Hz to 20 kHz +/- 3 dB (or more), change from baseline can indicate bulk movement of windings relative to each other. From 500 Hz to 2 MHz, changes of +/- 3 dB (or more) can indicate deformation within a winding. From 25 Hz to 10 MHz, changes of +/- 3 dB (or more) can indicate problems with winding leads and/or test leads placement. The above diagnostics come from the EuroDoble Client Committee after much testing experience and analysis. Note that there is a great deal of overlap in frequencies, which can mean more than one diagnosis."

The conclusion from comparing the definitions from the Cigré session 2004 and the Bureau of Reclamation instruction is that the frequency limits are guiding values. The reason for the variation is probably differences in statistical material, such as transformer ratings, transformer types and the amount of tested units. Conclusions regarding test leads depend upon the test equipment used.

Fig. 3.12 shows a typical response for a high voltage star connected winding. Different sub-bands are dominated [23] by different internal components of the transformer and are subsequently more sensitive to different types of failures, as summarized in Table 3.1.
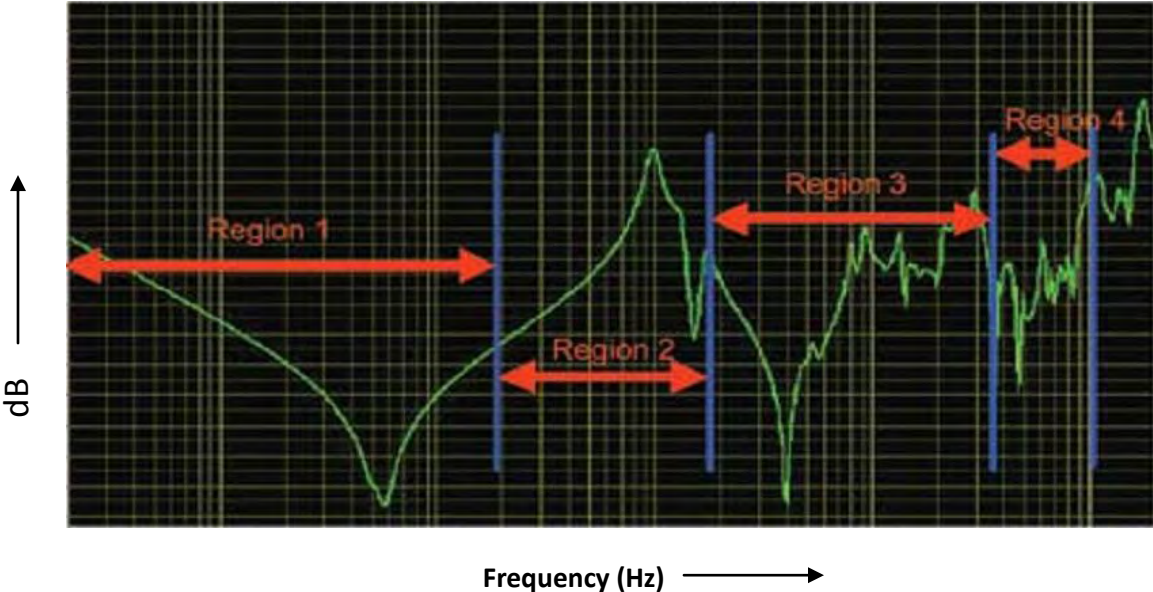
Figure 3.12: Frequency Analysis Bands

The method to define low, middle and high frequency ranges is however commonly accepted. A commonly accepted conclusion (from experience) is that frequency shifts (also small ones) between compared SFRA response curves is an indicator of serious fault conditions. Another conclusion is that difference in attenuation below 3 dB is often the result of irrelevant causes, and not an indication of serious damages.

Table 3.1: Frequency sub-band sensitivity

Region	Frequency Sub-Band	Component	Failure Sensitivity
1.	< 2 kHz	Main core bulk and winding inductance	Core deformation, open circuits, shorted turns and residual magnetism
2.	2 kHz to 20 kHz	Bulk component and shunt impedances	Bulk winding movement between windings and clamping structure
3.	20 kHz to 400 kHz	Main windings	Radial Deformation within the main or top windings
4.	400 kHz to 1 MHz	Main windings, top windings and internal leads	Axial Movement of the main & top winding, ground impedance variations

3.7   Motivation for SFRA Measurement

There are two distinct environments for application of sweep frequency response measurement: in the factory and in the field. In both cases the procedures and precautions used to generate a good measurement are the same. However, there is a difference in motivation for the tests in each category.

3.7.1   Factory Application

Reasons to use SFRA in a factory environment include:

a) Quality assurance
b) Baseline reference
c) Relocation and commissioning preparation

Manufacturers are using SFRA as part of their quality program to ensure transformer production is identical between units in a batch. The accuracy and repeatability of SFRA is the key to the program; the range from 20 Hz to 2 MHz is required to diagnose variations related to the core, the clamping structure, windings and leads.

An SFRA baseline can be produced in the factory when the transformer has been filled with oil and dressed as part of the factory commissioning tests. Many customers now appreciate the benefits of having a good baseline for SFRA measurements in the field when they need to respond to an incident. These customers require an SFRA measurement as part of their transformer purchase specification.

There are cases where a transformer is also tested in the factory without oil immediately prior to transport to the customer site. Some utilities specify that the transformer is shipped with small test bushings fitted to allow this test to take place. This allows the transformer to be tested as soon as it arrives on site without costly dressing and oil processing procedures. SFRA is safe to perform on a suitably prepared transformer without oil as the test is low voltage one.

3.7.2   Field Application

Reasons to use SFRA in a field environment include:

a) Relocation and commissioning validation
b) Post incident: lightning, fault, short circuit, seismic event etc

Once a transformer arrives on site after relocation it may be tested immediately, without oil if required, for comparison with baseline references or with sister units. (The provision of small test bushings prior to shipping aids in testing). This gives confidence in the mechanical integrity of the unit prior to commissioning. Some utilities prefer to check the impact recorders after the relocation and then, assuming no adverse impact recorder results are found, redo factory based SFRA tests once the transformer is dressed and ready for commissioning.

After a close up fault, or as a result of concern about the transformer from, for example, rising DGA levels, SFRA is a key tool in the engineer's toolbox for diagnosing the health of the transformer and its suitability for service. There is much to be gained in terms of information about mechanical integrity from an SFRA measurement, which supports evidence from Power Factor and Capacitance testing, Transformer Turns Ratio and Winding Resistance measurements.

Building a complete picture of the transformer from all available data is critical in making engineering judgments about an individual unit. Returning an unhealthy unit to service may prove catastrophic.

3.8   Fault Detection by SFRA

SFRA is able to detect a number of fault conditions, both mechanical and electrical. The main application of SFRA is to detect mechanical faults, for which some are detectable by SFRA only and some are useful to analyze both with SFRA and other methods for correlation. Electrical faults are often easy to detect using SFRA, but are also easily detectable by other methods.

Examples of fault conditions that can be detected by SFRA:

Mechanical faults:

    a) Winding deformations (including hoop buckling)
    b) Winding movement
    c) Partial collapse of winding
    d) Core displacements
    e) Broken or loosened winding or clamping structure

Electrical faults:

    a) Shorted turns or open circuit winding
    b) Bad ground connection of the transformer tank

3.9   Conclusion

SFRA is often the only method that can detect axial movements of a winding [10] as well as distortion or damage of transformer core. SFRA does also detect radial movements, which can be detected by leakage reactance tests (short-circuit impedance test) as well. It is useful to correlate the two methods to increase the precision of the result. This is also true for other faults, especially mechanical faults.

Chapter 4

Cross Correlation Co-Efficient (CCF)

4.1　Introduction

In statistics, *'Dependence'* refers to any statistical relationship between two random variables or two sets of data. Correlation refers to any of a broad class of statistical relationships involving dependence.

Familiar examples of dependent phenomena include the correlation between the physical statures of parents and their offspring or the correlation between the demand for a product and its price. Correlations are useful because they can indicate a predictive relationship that can be exploited in practice. For example, an electrical utility may produce less power on a mild day based on the correlation between electricity demand and weather. In this example there is a causal relationship, because extreme weather causes people to use more electricity for heating or cooling; however, statistical dependence is not sufficient to demonstrate the presence of such a causal relationship.

Formally, *'Dependence'* refers to any situation in which random variables do not satisfy a mathematical condition of probabilistic independence. In loose usage, *correlation* can refer to any departure of two or more random variables from independence, but technically it refers to any of several more specialized types of relationship between mean values. There are several correlation coefficients, often denoted ρ or r, measuring the degree of correlation. The most common of these is the Pearson correlation coefficient, which is sensitive only to a linear relationship between two variables (which may exist even if one is a nonlinear function of the other). Other correlation coefficients have been developed to be more robust than the Pearson Correlation — that is, more sensitive to nonlinear relationships.

4.2   Mathematical Expression

The most familiar measure of dependence between two quantities is the Pearson product-moment Correlation Coefficient, or "Cross Correlation Co-Efficient (CCF)". It is obtained by dividing the covariance of the two variables by the product of their standard deviations. Karl Pearson developed the coefficient from a similar but slightly different idea by Francis Galton.[4]

The Cross Correlation Co-Efficient $\rho_{X,Y}$ between two random variables X and Y with expected values μ_X and μ_Y and standard deviations σ_X and σ_Y is defined as:

$$\rho_{X,Y} = \operatorname{corr}(X,Y) = \frac{\operatorname{cov}(X,Y)}{\sigma_X \sigma_Y} = \frac{E[(X - \mu_X)(Y - \mu_Y)]}{\sigma_X \sigma_Y},$$

where E is the expected value operator, *cov* means covariance, and, *corr* a widely used alternative notation for Pearson's correlation.

The Pearson correlation is defined only if both of the standard deviations are finite and both of them are nonzero. It is a corollary of the Cauchy–Schwarz inequality that the correlation cannot exceed 1 in absolute value. The correlation coefficient is symmetric: $\operatorname{corr}(X,Y) = \operatorname{corr}(Y,X)$. The Pearson correlation is +1 in the case of a perfect positive (increasing) linear relationship (correlation), −1 in the case of a perfect decreasing (negative) linear relationship (Anti-Correlation),[5] and some value between −1 and 1 in all other cases, indicating the degree of linear dependence between the variables. As it approaches zero there is less of a relationship (closer to uncorrelated). The closer the coefficient is to either −1 or 1, the stronger the correlation between the variables.

If the variables are independent, Pearson's correlation coefficient is 0 but the converse is not true because the correlation coefficient detects only linear dependencies between two variables. For example, suppose the random variable X is symmetrically distributed about zero, and $Y = X^2$. Then Y is completely determined by X, so that X and Y are perfectly dependent, but their correlation is zero; they are uncorrelated. However, in the special case when X and Y are jointly normal, un-correlatedness is equivalent to independence.

If we have a series of n measurements of X and Y written as x_i and y_i where $i = 1, 2, ..., n$, then the *Sample Cross Correlation Co-Efficient* can be used to estimate the population Pearson correlation r between X and Y. The Sample Cross Correlation Co-Efficient is written as

$$r_{xy} = \frac{\sum_{i=1}^{n}(x_i - \bar{x})(y_i - \bar{y})}{(n-1)s_x s_y} = \frac{\sum_{i=1}^{n}(x_i - \bar{x})(y_i - \bar{y})}{\sqrt{\sum_{i=1}^{n}(x_i - \bar{x})^2 \sum_{i=1}^{n}(y_i - \bar{y})^2}},$$

where x and y are the sample means of X and Y, and s_x and s_y are the sample standard deviations of X and Y.

This can also be written as:

$$r_{xy} = \frac{\sum x_i y_i - n\bar{x}\bar{y}}{(n-1)s_x s_y} = \frac{n\sum x_i y_i - \sum x_i \sum y_i}{\sqrt{n\sum x_i^2 - (\sum x_i)^2}\sqrt{n\sum y_i^2 - (\sum y_i)^2}}.$$

If x and y are measurements that contain measurement error, as commonly happens in biological systems, the realistic limits on the correlation coefficient are not -1 to +1 but a smaller range.

4.3 MATLAB code for Cross Correlation

The following MATLAB code has been developed in this thesis to calculate the Cross Correlation Co-Efficient (CCF) between two series. The two series are x[], and y[] of "n" points.

```
   int i,j
   double mx,my,sx,sy,sxy,denom,r;

/* Calculate the mean of the two series x[], y[] */

   mx = 0;
   my = 0;
   for (i=0;i<n;i++) {
       mx += x[i];
```

```
        my += y[i];
    }
    mx /= n;
    my /= n;


/* Calculate the denominator */

    sx = 0;
    sy = 0;
    for (i=0;i<n;i++) {
        sx += (x[i] - mx) * (x[i] - mx);
        sy += (y[i] - my) * (y[i] - my);
    }
    denom = sqrt(sx*sy);


/* Calculate the correlation series */

    for (delay=-maxdelay;delay<maxdelay;delay++) {
        sxy = 0;
        for (i=0;i<n;i++) {
            j = i + delay;
            if (j < 0 || j >= n)
                continue;
            else
                sxy += (x[i] - mx) * (y[j] - my);
            /* Or should it be (?)
            if (j < 0 || j >= n)
                sxy += (x[i] - mx) * (-my);
            else
                sxy += (x[i] - mx) * (y[j] - my);
            */
        }
        r = sxy / denom;

        /* r is the correlation coefficient at "delay" */

    }
```

If the series are considered circular then the source with the same declarations as above might be

```
/* Calculate the mean of the two series x[], y[] */

    mx = 0;
    my = 0;
    for (i=0;i<n;i++) {
        mx += x[i];
        my += y[i];
    }
```

```
    mx /= n;
    my /= n;


/* Calculate the denominator */

    sx = 0;
    sy = 0;
    for (i=0;i<n;i++) {
        sx += (x[i] - mx) * (x[i] - mx);
        sy += (y[i] - my) * (y[i] - my);
    }
    denom = sqrt(sx*sy);


/* Calculate the correlation series */

    for (delay=-maxdelay;delay<maxdelay;delay++) {
        sxy = 0;
        for (i=0;i<n;i++) {
            j = i + delay;
            while (j < 0)
                j += n;
            j %= n;
            sxy += (x[i] - mx) * (y[j] - my);
        }
        r = sxy / denom;

        /* r is the correlation coefficient at "delay" */

    }
```

4.4 MATLAB code for Curve Point Extraction

```matlab
clc;
clear all;

pic=imread('3.jpg');


%%%%%%%%%%%%%%%%%%%%%%%%%%%%%%%%%%%%%%%%%%%%%%%%%%%%%%%%%%%%%%%%

startX = 56;
startY = 66;
endX = 1007;

% AT FIRST, THE (0,0) POINT OF THE GRAPH HAVE TO FIND MANUALLY.
% THE FIGURE WHICH WILL BE LOADED FIRST HAVE TO BE ZOOMED.
```

```matlab
% THE VALUE OF startX AND startY WILL BE THE CO-ORDINATE VALUES OF X
AND Y
% THE VALUE OF THE X CO-ORDINATE AT THE LAST END OF THE CURVE WILL
HAVE TO BE ASSIGNED AS VALUE OF endX
% MUST HAVE TO KEEP IN MIND THAT THE VALUE OF startX WILL BE JUST 1
PIXEL AFTER OF THE 1ST POINT AND THE VALUE OF endX WILL BE JUST 1 PIXEL
BEFORE THE LAST POINT.
% OTHERWISE THE BLACK LINE WILL CREATE PROBLEM

%%%%%%%%%%%%%%%%%%%%%%%%%%%%%%%%%%%%%%%%%%%%%%%%%%%%%%%%%%%%%%%%%%

YupperLimit = 200;
YlowerLimit = 51;

% AT THE TIME OF DEFINING UPPER AND LOWER LIMIT, MUST HAVE TO KEEP IN
MIND THAT POINT EXTRACTION SHOULD NOT GO BEYOND THE TWO BLACK
BOUNDARY.
% IF THERE LAYS ANY BLABK LINE OR WRITING IN THE GRAPH THEN IT HAS TO
BE REMOVED USING PAINT.

%%%%%%%%%%%%%%%%%%%%%%%%%%%%%%%%%%%%%%%%%%%%%%%%%%%%%%%%%%%%%%%%%%%%%

standardValuepixel = 169;
standardValue = -60;


StartTime = 0;
EndTime = 100;

% START AND ENDING TIME HAS TO BE DEFINED
%%%%%%%%%%%%%%%%%%%%%%%%%%%%%%%%%%%%%%%%%%%%%%%%%%%%%%%%%%%%%%%%%%%%%%%%

COMPVALUE = 150


Time = (startX:endX)-startX;
Time = EndTime*Time/Time(end);


pic2 = pic;
pic2(startY:startY,startX:endX,1) = 255;
pic2(startY:startY,startX:endX,2) = 0;
pic2(startY:startY,startX:endX,3) = 0;

pic2(YupperLimit:YupperLimit,startX:endX,1) = 255;
pic2(YupperLimit:YupperLimit,startX:endX,2) = 0;
pic2(YupperLimit:YupperLimit,startX:endX,3) = 0;

pic2(YlowerLimit:YlowerLimit,startX:endX,1) = 255;
pic2(YlowerLimit:YlowerLimit,startX:endX,2) = 0;
pic2(YlowerLimit:YlowerLimit,startX:endX,3) = 0;
```

```
imview(pic2);


data = double(pic);

data = data(:,:,1)+data(:,:,2)+data(:,:,3);

data = uint8(data);
value1 = zeros(1,endX-startX+1);
value 2= zeros(1,endX-startX+1);


found = value1;
index = 1;
for index1 = startX:endX
  for index2 = YupperLimit:-1:YlowerLimit
   if(data(index2,index1)<COMPVALUE)
   value1(index) = index2;
   found(index) = 1;
   end
  end
index = index+1;
end
value1 = (value1-startY);


found = value2;
index = 1;
for index1 = startX:endX
  for index2 = YlowerLimit:1:YupperLimit
   if(data(index2,index1)<COMPVALUE)
   value2(index) = index2;
   found(index) = 1;
   end
  end
index = index+1;
end
value2 = (value2-startY);

value = (value1+value2)/2;

value = value*standardValue/(standardValuepixel-startY);

figure(2)
plot(Time,value)
grid on
```

Chapter 5

Transformer Condition Assessment Through Traditional Response Analysis Method

5.1   Traditional Method

In traditional method, the interpretation of frequency response curves depends on Transformer Testing Engineers' experience. In this method, response curve of the transformer is taken at the manufacturing factory. Then after transportation or relocation at concern site, the response curve is measured again. An experienced observer then examines the two curves for any significant differences. Significant differences are usually understood to be:

a) Changes to the shape of the curve
b) The creation of new resonant frequencies or the elimination of existing resonant frequencies
c) Large shifts in existing resonant frequencies [9].

The main problem with these methods of comparison is that the expert's opinion may lack both objectivity and transparency. One way of addressing both problems is to note down all of the resonant frequencies. This gives specific and transparent information on the number of resonances that have been created or eliminated and how far any resonances may have shifted.

For any transformer, if the response curves from the manufacturing industry is unavailable then response curve is taken from a transformer of same rating and design. This new transformer of same rating and design with respect to the previous one is known as Sister Transformer and its response curve are considered as ‗Reference' to make the comparison with the suspected transformer.

Three case studies have been represented here to demonstrate how condition assessment is done through traditional method:

Table 5.1: Case study for traditional fault diagnosis method

Case	Capacity MVA	HT Voltage kV	LT Voltage kV	Phase	Year of Manufacture	Country of Origin
1	50	132	11	3	2010	Bangladesh
2	25	132	11	1	2009	Bangladesh
3	80	230	11	3	2011	China

5.2 Case 1: 50 MVA, 132/11 kV Power Transformer at 132 kV Substation

This 40/50 MVA transformer (vector group YNd-1) was manufactured by Energypac Engineering Ltd. for 132 kV substation of 102 MW power generation plant established by Summit Power Ltd. Appendix – A.1 and A.2 gives more detail data. Before dispatch from the manufacturing industry, SFRA measurements were taken on the HV windings keeping the LV windings open for all the three phase. Then the measurements were repeated on HV windings keeping LV windings shorted for all the three phases. After that, LV response for three phases was taken while all HV terminals were kept open.

On the way to power plant from manufacturing factory, it had to face several critical jerking at the time of vehicle interchanging. It was sent by truck-lorry followed by cargo ferry. At the site, an SFRA reading was taken to determine whether any mechanical displacement has taken place in the active part or not. Using the recommended table for analyzing (Table-3.1), it was found that all the 4 regions are within good limit and further investigation was unnecessary. There is no severe change in the shape of curves, no creation of new resonant frequencies or no the elimination of existing resonant frequencies as well as no large shifts in existing resonant frequencies. All the ―Magnitude vs. Frequency" plots have been shown at Figure 4.1, 4.2, 4.3, 4.4, 4.5 and 4.6. From an expert's eye view, the transformer was healthy enough to energize at line and it is working without any trouble.

Figure 5.1: HV windings responses keeping the LV windings open (at manufacturing factory)

Figure 5.2: HV windings responses keeping the LV windings open (at concern site)

Figure 5.3: HV windings responses keeping the LV windings shorted (at manufacturing factory)

Figure 5.4: HV windings responses keeping the LV windings shorted (at concern site)

Figure 5.5: LV windings responses keeping the HV windings open (at manufacturing factory)

Figure 5.6: LV windings responses keeping the HV windings open (at concern site)

5.3 Case 2: 25 MVA, 132/11 kV Power Transformer at 132 kV Substation

This 20/25 MVA, single phase transformer was manufactured by Energypac Engineering Ltd. for 132 kV substation of 50 MW power generation plant established by Energypac Power Generation Ltd. Appendix – A.3 gives more detail data. Like the previous case, before dispatch from the manufacturing industry, SFRA measurements were taken on the HV windings keeping the LV windings open. Then the measurements were repeated on HV windings keeping LV windings shorted. At last, LV response was taken while all HV terminals were kept open.

On the way to power plant from manufacturing factory, this transformer aslo had to face several critical jerking at the time of vehicle interchanging as it was sent by truck-lorry followed by cargo ferry. At the site, an SFRA reading was taken to determine whether any mechanical displacement has taken place in the active part or not. As it is a single phase transformer, so instead of getting three curves for three phases, we have got only one response curve for each combination of connection. Through this data shortage, in order make better prediction; Phase response curve has been collected for each combination according with Magnitude response curve. Using the recommended table for analyzing (Table-3.1), it was found that all the 4 regions are within good limit and further investigation was unnecessary. There is no severe change in the shape of curves, no creation of new resonant frequencies or no the elimination of existing resonant frequencies as well as no large shifts in existing resonant frequencies in both ―Magnitude vs. Frequency‖ and ―Phase vs. Frequency‖ curves. All the ―Magnitude vs. Frequency‖ and ―Phase vs. Frequency‖ plots have been shown at Figure 4.7, 4.8, 4.9 and 4.10. According to expert‗s testing result, the transformer was healthy enough to energize at line and it is working properly.
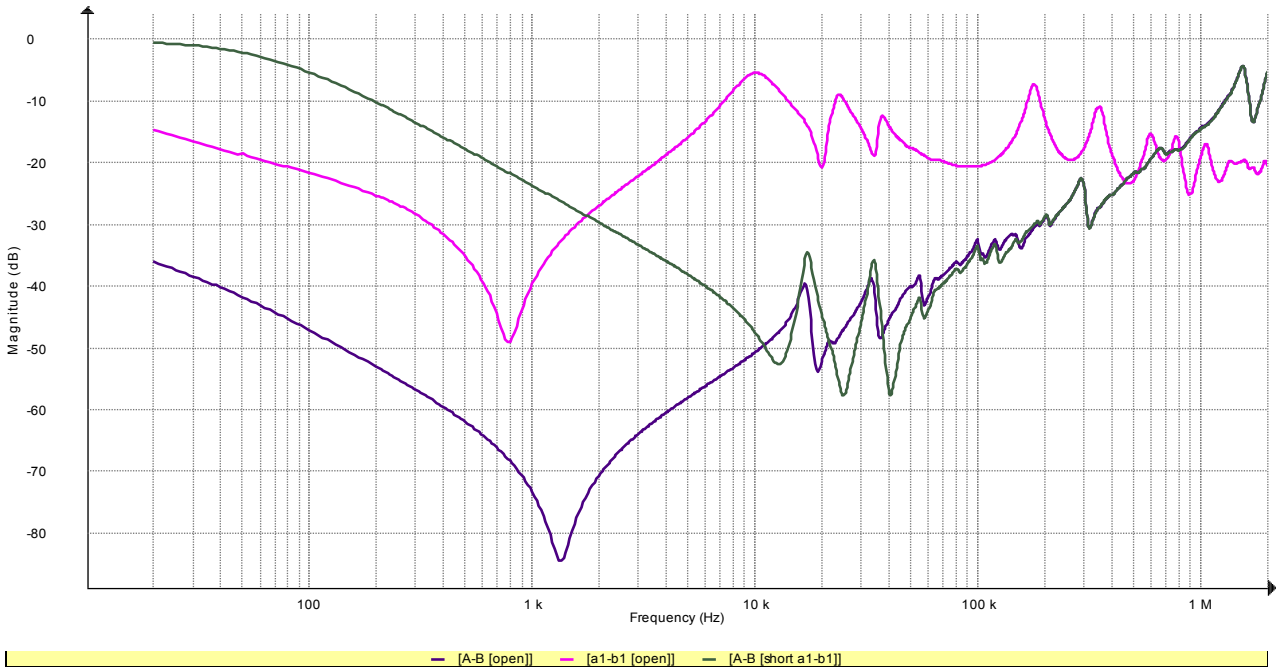
Figure 5.7: HV & LV windings Magnitude Responses at different winding connections (at manufacturing factory)
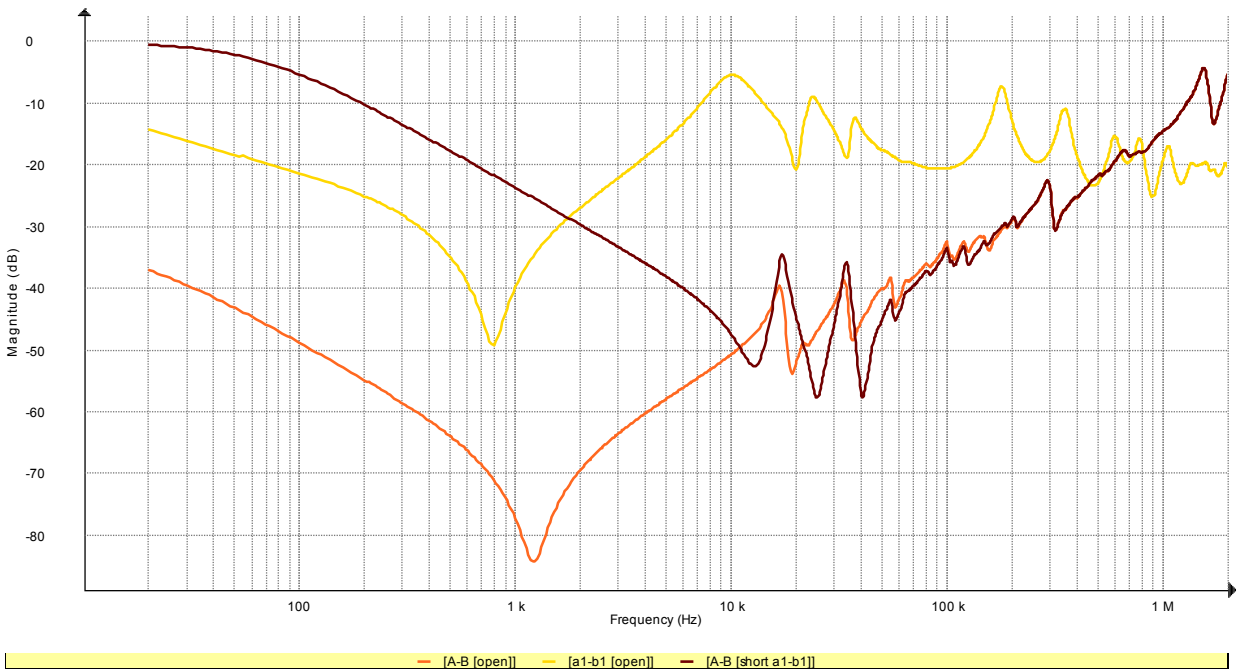
Figure 5.8: HV & LV windings Magnitude responses at different winding connections (at concern site)
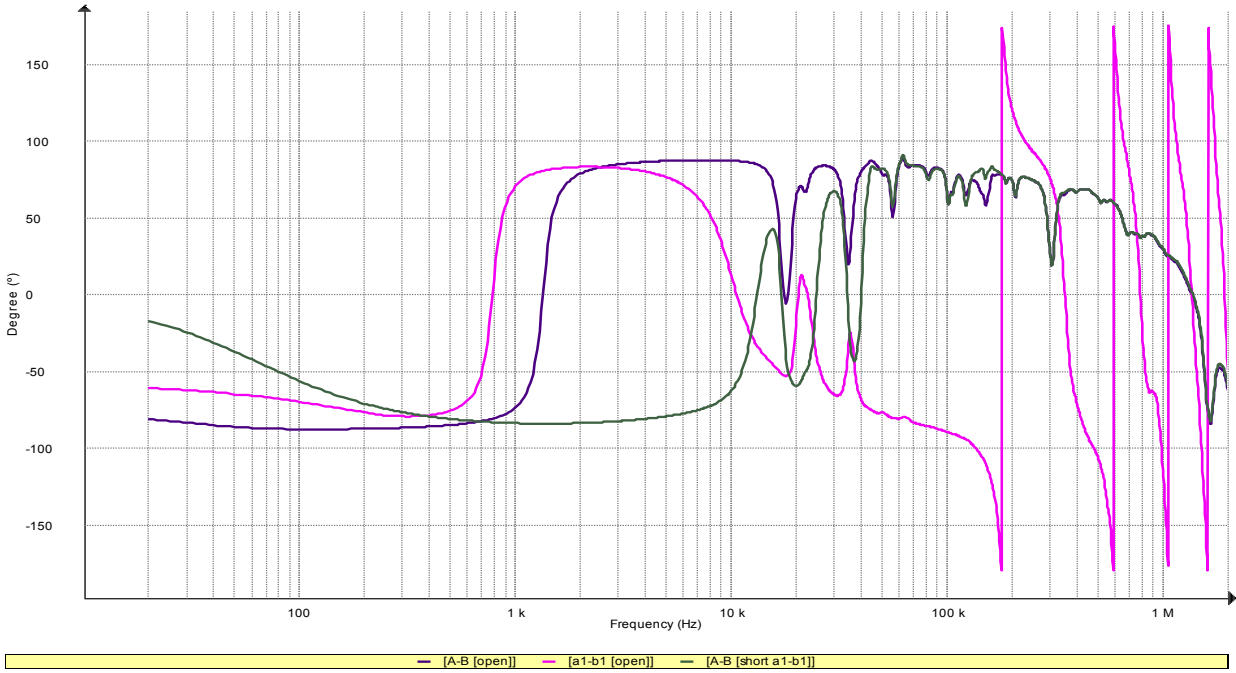
Figure 5.9: HV & LV windings Phase Responses at different winding connections (at manufacturing factory)
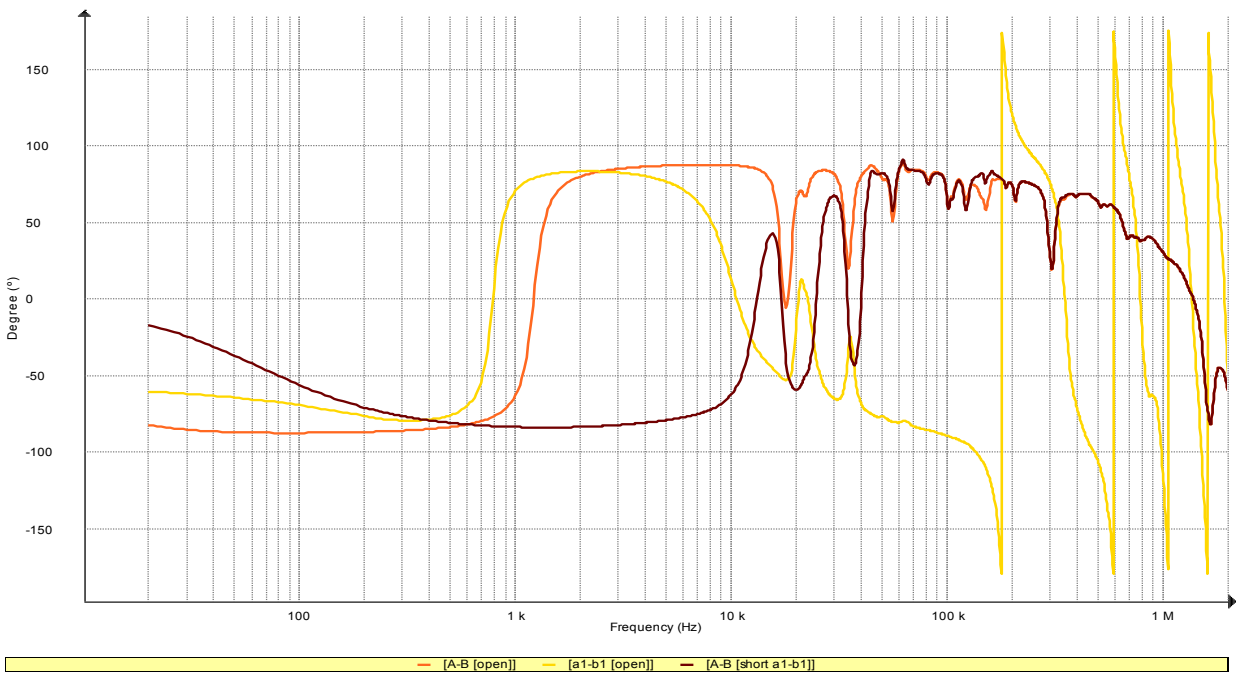
Figure 5.10: HV & LV windings Phase responses at different winding connections (at concern site)

5.4 Case 3: 80 MVA, 230/11 kV Power Transformer at 230 kV Substation

This 70/80 MVA, three phase (vector group YNd-1) transformer was manufactured by Sanbian Sci-Tech Co. Ltd. for 230 kV substation of 65 MW power generation plant established by United Generation & Transmission Company Ltd. At the manufacturing industry, SFRA measurement of the transformer was not taken by the Chinese engineers due to unavailability of SFRA machine set-up. As a result, no primary response from the manufacturing factory was available to regard as ‗Standard Response' and to compare.

This transformer was sent by ship from China to Bangladesh. At the Chittagong port, it was shifted to a smaller ship from the foreign vessel. Finally at Ashuganj port, the transformer was shifted to a truck-lorry to its final destination power plant. At the site, an SFRA reading was taken to detect probable mechanical deformation taken place in the active part or not. Using the recommended table for analyzing (Table-3.1), it was found that the first three regions are within good limit. So no mechanical damage at Core, Inter Winding distance as well no deformation of main windings due to radial movement. But in region 4 (400 kHz ~ 1 MHz), the HV winding response of Phase-B has been deviated severely with respect to Phase-A and Phase-C responses. This deviation is clearly viewable at Figure 4.11. As a result, no doubt to tell about that Phase-B of High Voltage winding has become deformed due to axial force. All the ―Magnitude vs. Frequency‖ plots have been shown at Figure 4.11, 4.12 and 4.13. From Figure 4.13, it's visible that all three responses from three LV windings are similar. So all the Low Voltage windings are at healthy condition and not severely deformed. This transformer was marked as faulty one and has been sent back to China for repairing.
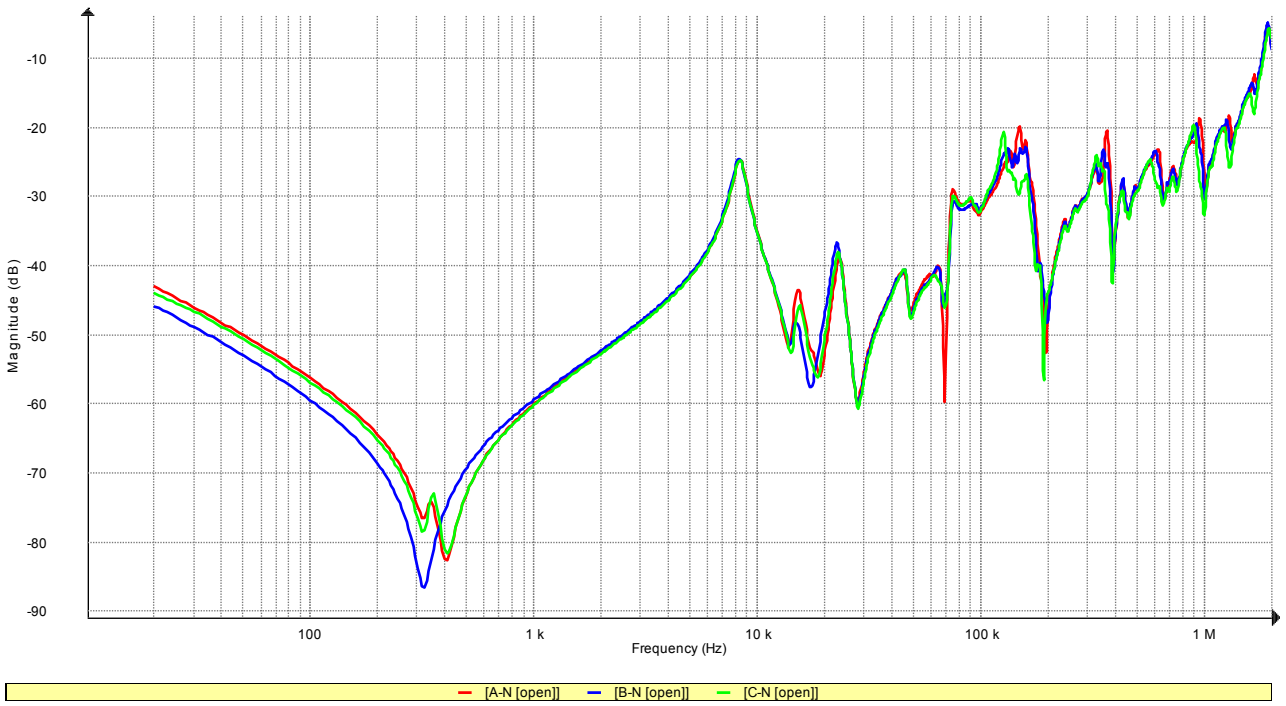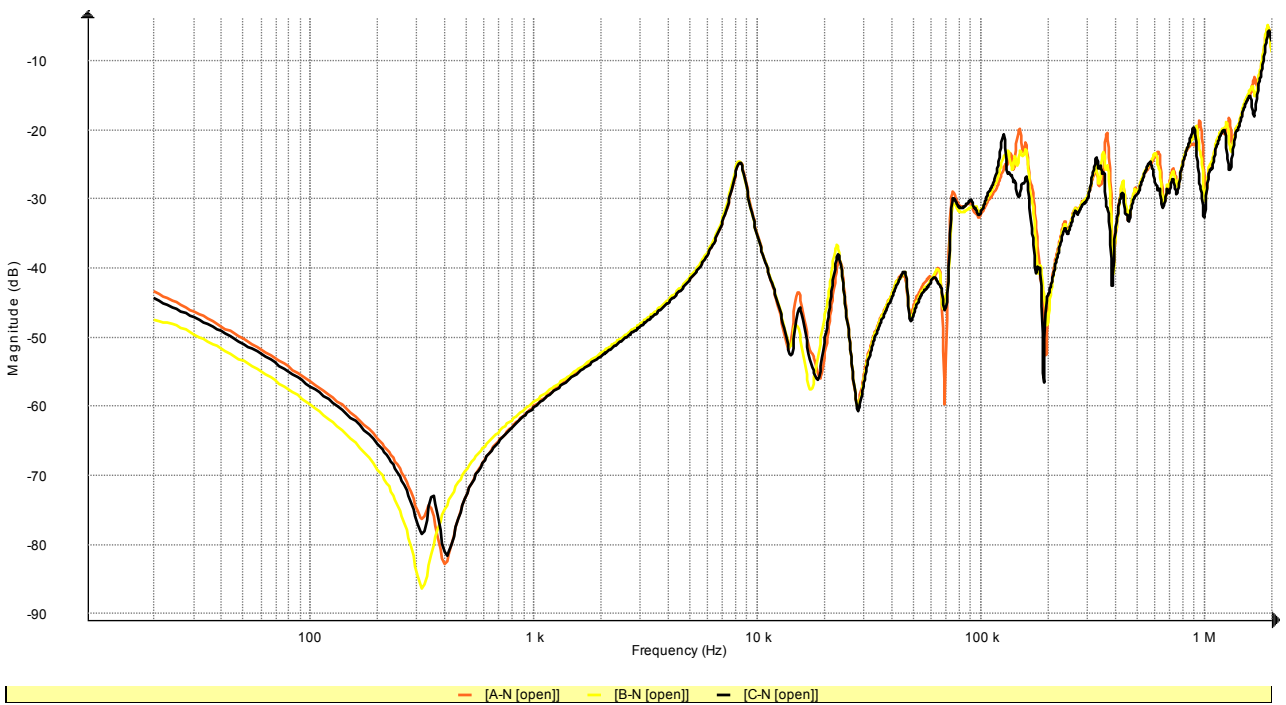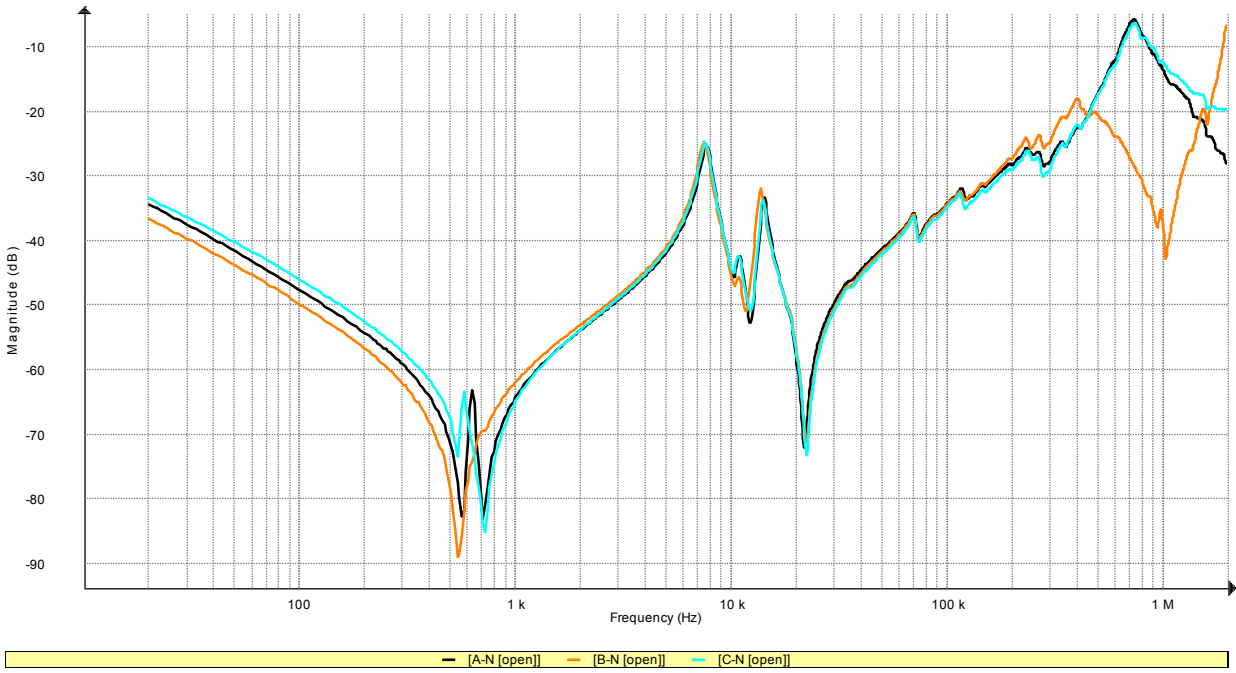
Figure 5.11: HV windings responses keeping the LV windings open (at concern site)
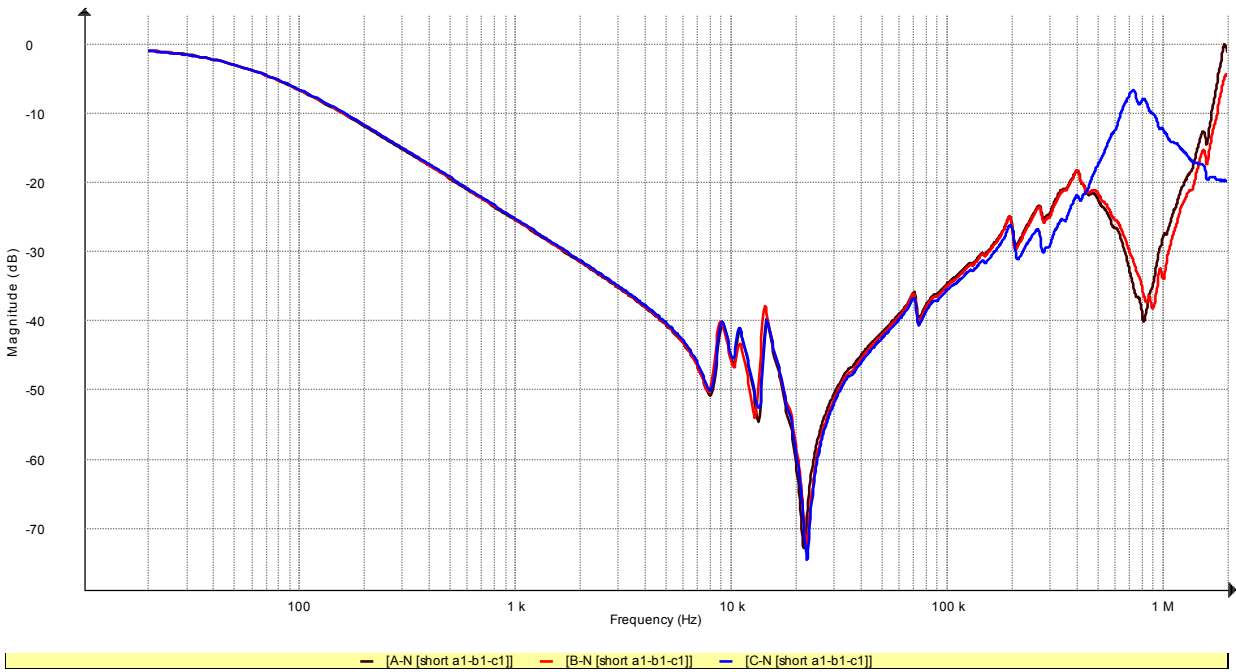
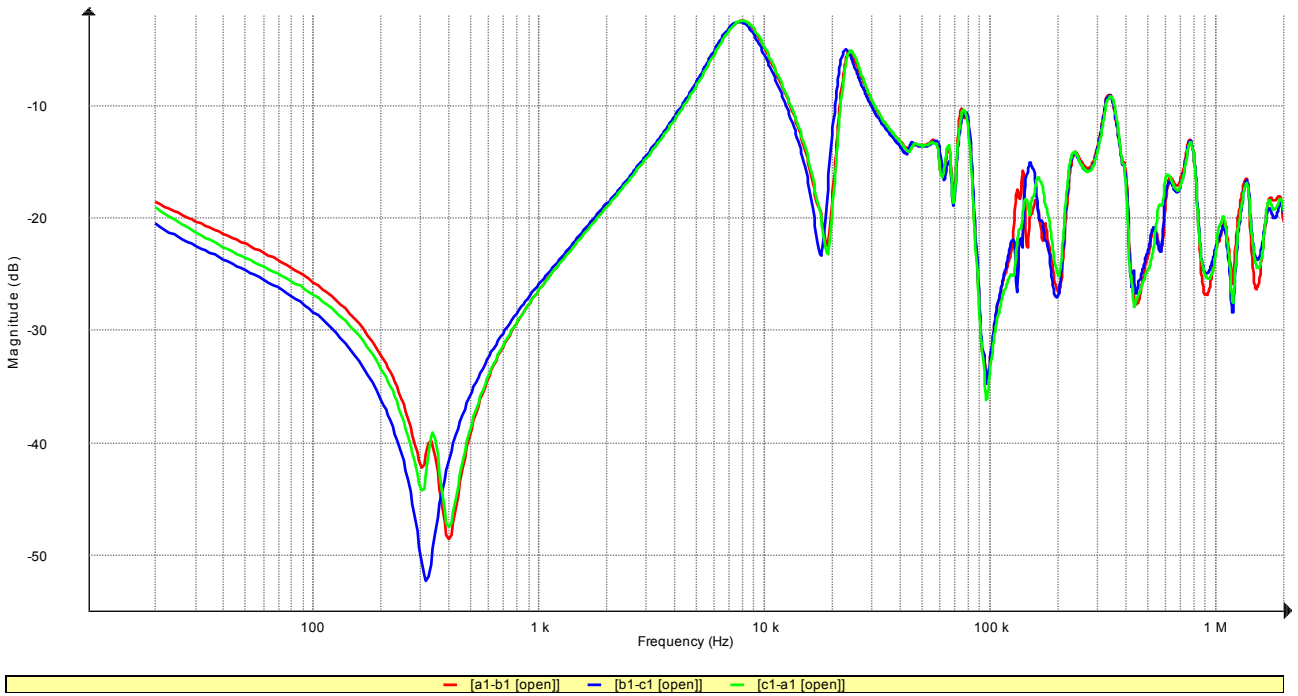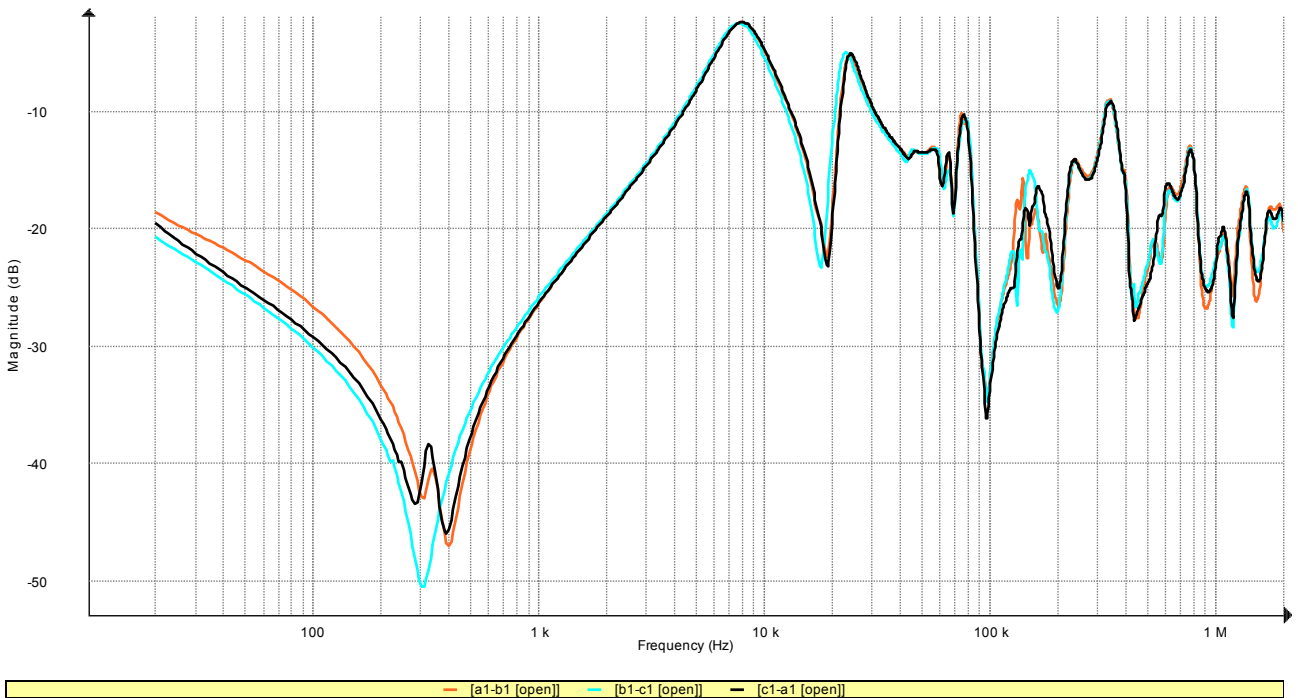Figure 5.12: HV windings responses keeping the LV windings Shorted (at concern site)

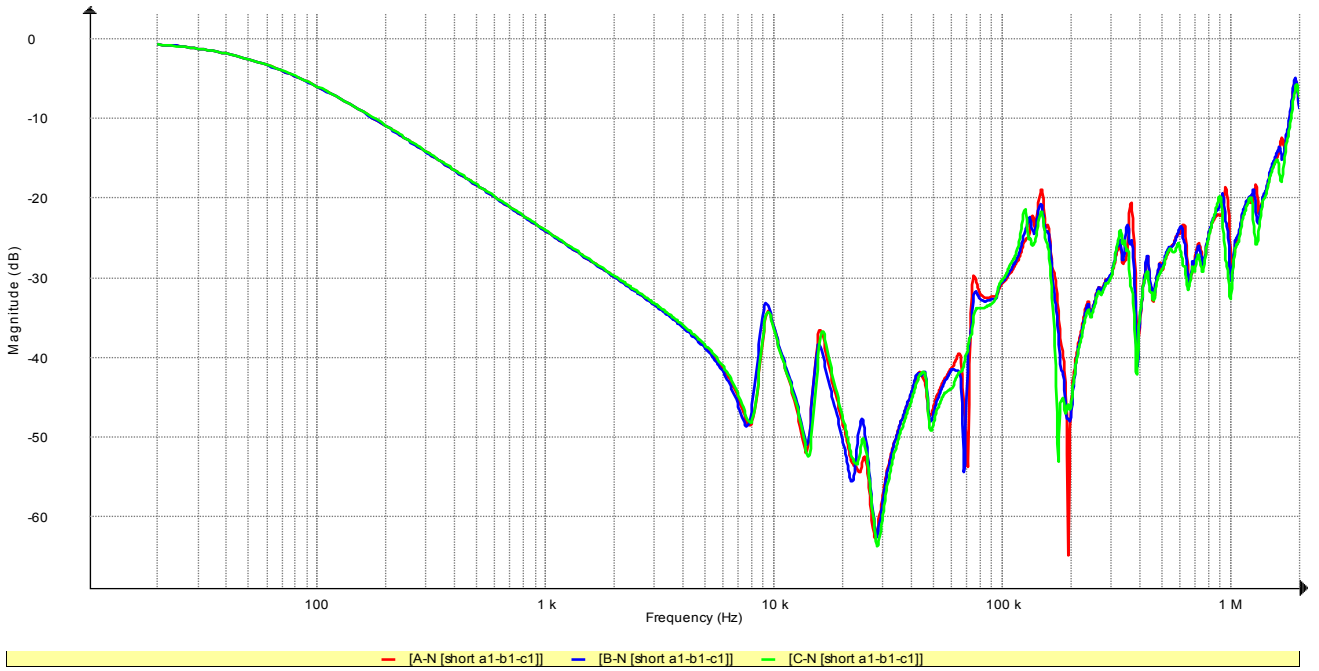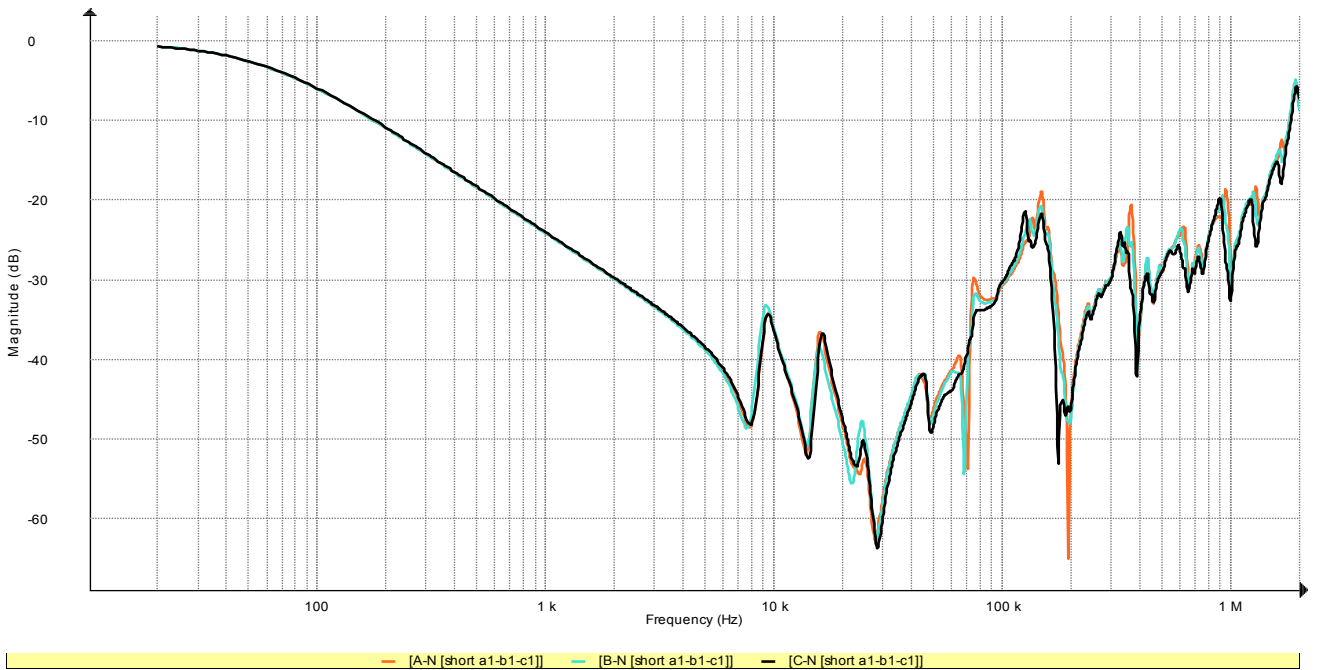Figure 5.13: LV windings responses keeping the HV windings open (at concern site)

Chapter 6

Fault Detection using Cross Correlation Co-Efficient

6.1   Implementation of CCF

In order to show the effectiveness of Cross Correlation Co-Efficient (CCF) measurement method for fault detection in power transformers, three case studies of faulty transformers has been considered and fault type as well as location of the fault in these transformers has been predicted using CCF calculation results. After calculative prediction, each transformer has been opened to verify the outcome.

The brief information about these case studies are described in table 6.1

Table 6.1: Case studies for fault detection

Case	Capacity MVA	HT Voltage kV	LT Voltage kV	Phase	Year of Manufacture	Country of Origin
1	14	33	11.6	3	1991	England
2	41.67	132	33	3	1998	India
3	80	132	11	3	2011	China

6.2   Case 1: 14 MVA, 33/11.6 kV, 3φ Power Transformer at 33 kV Substation

The subjected transformer was running at Dhaka Power Distribution Company (DPDC). It is a 10/14 MVA, 33/11.6 kV (vector group - YNd11) power transformer manufactured by Brush Transformers Ltd. (Loughborough, England) at 1991. Appendix A.4 gives more specific data. Due to its age of 20 years, frequency response of this transformer was taken to predict its aging effect. At first, test was carried on HV side keeping LV side open followed by LV side shorted. Corresponding Bode Plot response has been shown in figure 6.1 and 6.2. CCF results are shown in Table 6.2 and 6.3.
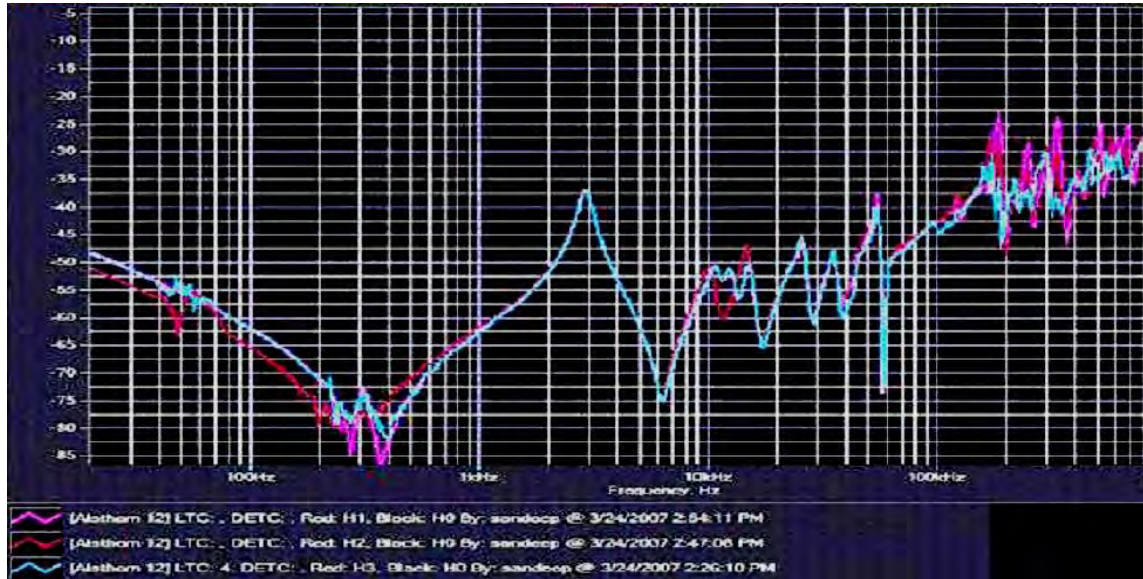
Figure 6.1: HV winding response (LV open)

Table 6.2: CCF of HV winding keeping LV open

Frequency Sub-band	CCF results		
	X1-X0, X2-X0	X2-X0, X3-X0	X3-X0, X1-X0
0 – 2 kHz	0.7981	0.7825	0.9914
2 kHz – 20 kHz	0.9743	0.9841	0.9736
20 kHz – 400 kHz	0.9523	0.9267	0.9081
400 kHz – 1 MHz	0.8394	0.8975	0.8427
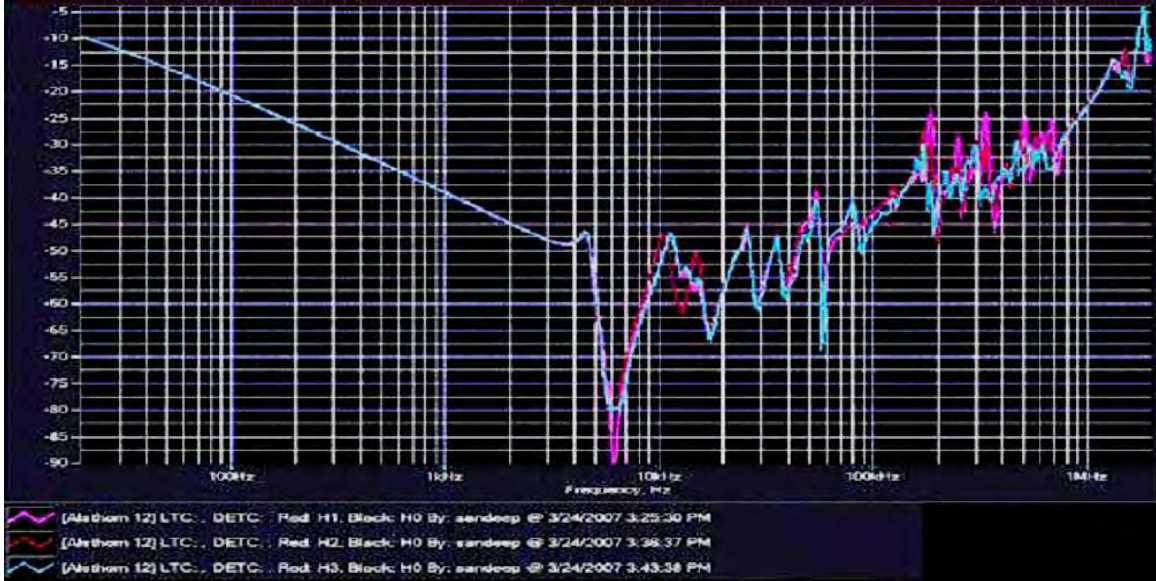
Figure 6.2: HV winding response (LV short)

Table 6.3: CCF of HV winding keeping LV short

Frequency Sub-band	CCF results		
	X1-X0, X2-X0	X2-X0, X3-X0	X3-X0, X1-X0
0 – 2 kHz	0.9981	0.9925	0.9954
2 kHz – 20 kHz	0.9743	0.9861	0.9786
20 kHz – 400 kHz	0.9354	0.9283	0.9217
400 kHz – 1 MHz	0.8113	0.8671	0.8039

From the CCF result (Table-6.2 & 6.3), it is easily viewable that the matching is very poor at low frequency region (0-2 kHz). This may be due to core deformation as a result of axial stress because the transformer is running for a long time (20 years). Again, poor matching at higher region (400 kHz-1 MHz) indicates main coil deformation either by radial stress or by axial stress. This deformation is more severe for A phase (Red phase).
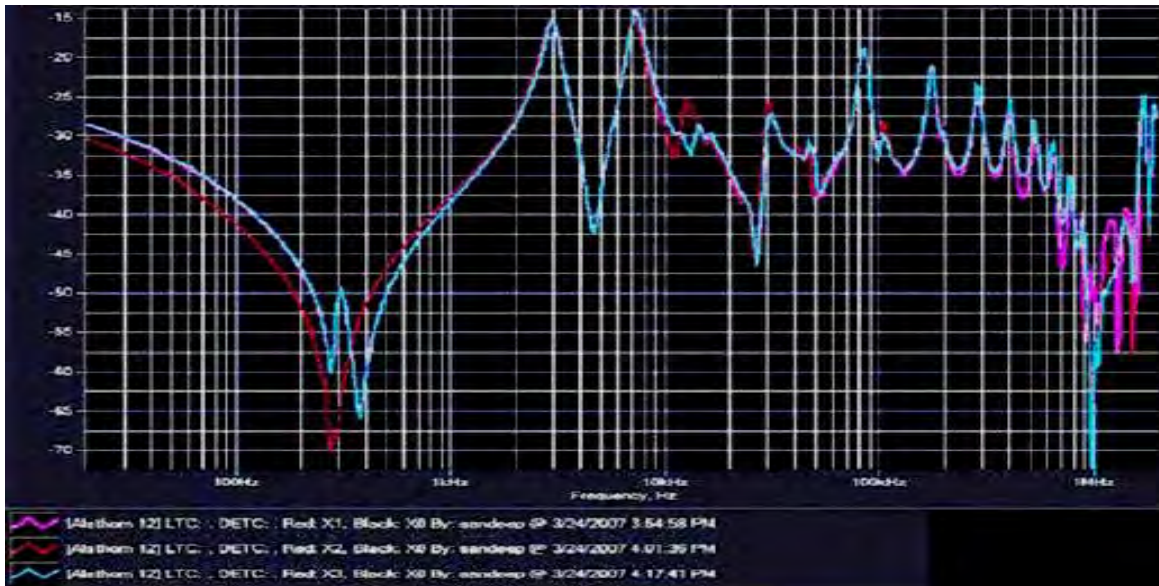
Figure 6.3: LV winding response (HV open)

Table 6.4: CCF of LV winding keeping HV open

Frequency Sub-band	CCF results		
	X1-X0, X2-X0	X2-X0, X3-X0	X3-X0, X1-X0
0 – 2 kHz	0.8381	0.8325	0.9907
2 kHz – 20 kHz	0.9943	0.9921	0.9936
20 kHz – 400 kHz	0.9825	0.9867	0.9781
400 kHz – 1 MHz	0.8493	0.9275	0.8027

From LV winding response (Figure 6.3) and corresponding CCF calculation (Table 6.4), the previous assumption becomes stronger. Poor matching at low frequency region (0-2 kHz) and high frequency region (400 kHz-1 MHz) again spans the prediction of core damage and main winding movement firmly. After replacing the transformer from the system, it was dissected and both the prediction became true. The corresponding core and coil of this transformer is shown in figure 6.4 and 6.5.

Figure 6.4: The position of the fault in the Core structure

Figure 6.5: The damaged coil of HV A-phase (Red phase)

6.3 Case 2: 41.67 MVA, 132/33 kV, 3φ Power Transformer at 132 kV Substation

The results here are from a three phase 25/41.67 MVA, 132/33 kV (vector group Dyn-1) power transformer manufactured by EMCO Transformers Ltd. (Maharastra, India) at 1998 for Bangladesh Power Development Board (BPDB) 132 kV sub-station. Appendix A.5 gives more specific data. The transformer had tripped out of service on protection. No reference factory results were available for this unit. So SFRA test was carried on it at the ―High Voltage Testing Laboratory‖ of Energypac Engineering Ltd. At first, test was carried on HV side keeping LV side open followed by LV side shorted. Corresponding Bode Plot response has been shown in figure 6.6 and 6.7. CCF results are shown in Table 6.5 and 6.6.
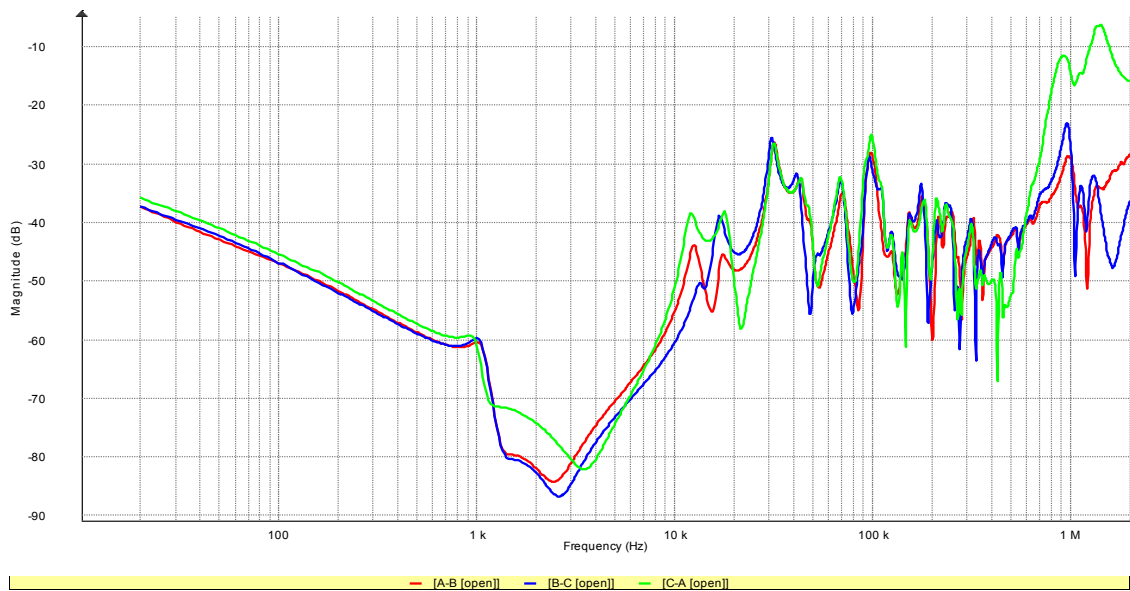
Figure 6.6: HV winding response (LV open)

Table 6.5: CCF of HV winding keeping LV open

Frequency Sub-band	CCF results		
	X1-X2, X2-X3	X2-X3, X3-X1	X3-X1, X1-X2
0 – 2 kHz	0.999	0.997	0.997
2 kHz – 20 kHz	0.968	0.949	0.958
20 kHz – 400 kHz	0.762	0.781	0.836
400 kHz – 1 MHz	0.997	0.947	0.948
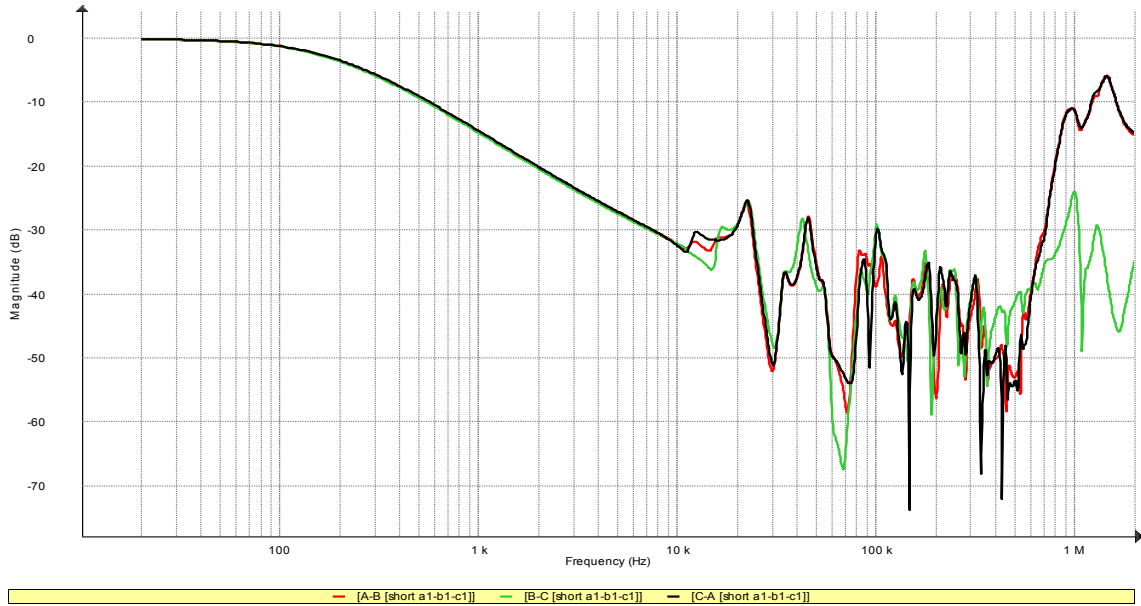
Figure 6.7: HV winding response (LV short)

Table 6.6: CCF of HV winding keeping LV short

Frequency Sub-band	CCF results		
	X1-X2, X2-X3	X2-X3, X3-X1	X3-X1, X1-X2
0 – 2 kHz	0.999	0.999	0.999
2 kHz – 20 kHz	0.985	0.959	0.99
20 kHz – 400 kHz	0.849	0.813	0.854
400 kHz – 1 MHz	0.948	0.942	0.981

From the CCF result (Table-6.5 & 6.6), it is easily viewable that the matching is very close at low frequency region (0-2 kHz). This indicates that the core of this transformer is very good condition according with the core bolts and channels. But, very poor matching at the 20 kHz – 400 kHz band indicates that high voltage coil is severely deformed or damaged specifically due to radial force. This deformation is severe for all three phases.
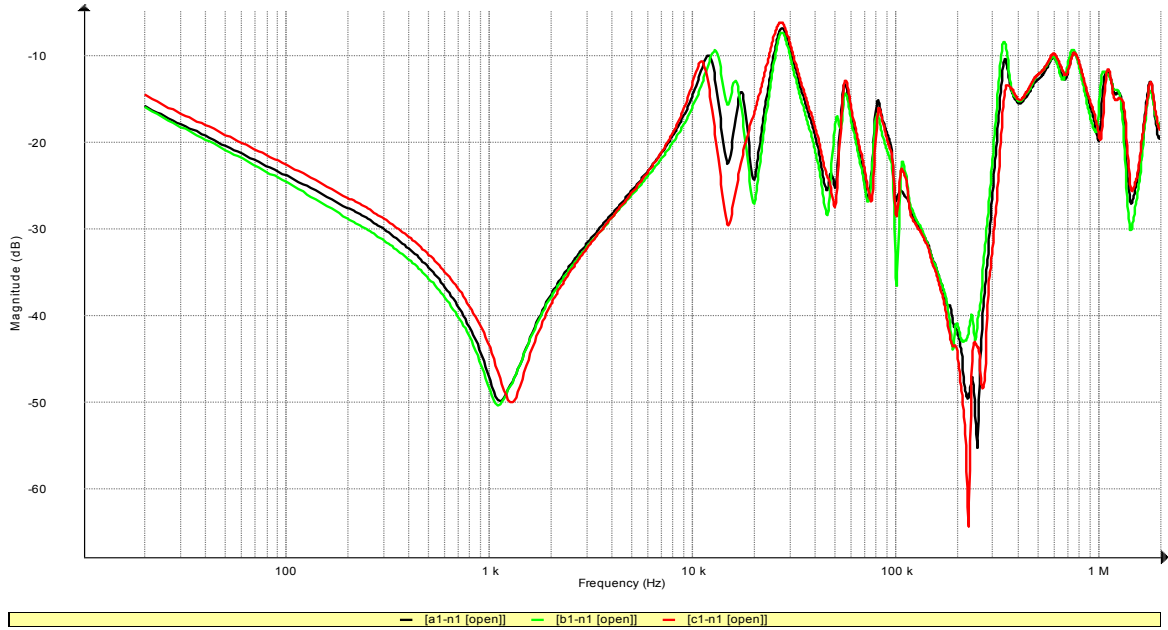
Figure 6.8: LV winding response (HV open)

Table 6.7: CCF of LV winding keeping HV open

Frequency Sub-band	CCF results		
	X1-X0, X2-X0	X2-X0, X3-X0	X3-X0, X1-X0
0 – 2 kHz	0.996	0.999	0.995
2 kHz – 20 kHz	0.961	0.819	0.931
20 kHz – 400 kHz	0.972	0.924	0.965
400 kHz – 1 MHz	0.965	0.957	1.000

From LV winding response (Figure 6.8) and corresponding CCF calculation (Table 6.7), the previous assumption becomes stronger. Very close matching at low frequency region (0-2 kHz) again spans the prediction of healthy core condition firmly. As well as, close/good matching value of CCF in all other regions indicate undamaged or undistorted Low Voltage windings. At the factory of Energypac, it was opened for repairing and both the prediction became true. The corresponding core and coil of this transformer is shown in figure 6.9 and 6.10.

Figure 6.9: Damaged HV (phase-C) coil
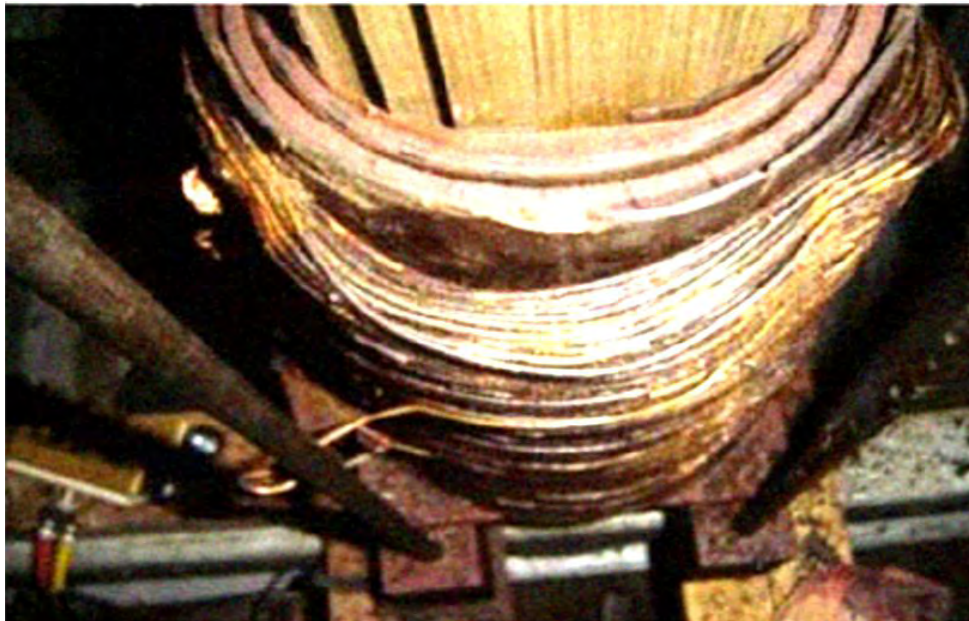
Figure 6.10: Coil deformation due to Radial Stress

6.4   Case 3: 80 MVA, 230/11 kV Power Transformer at 230 kV Substation

This is the last case of fourth chapter. This 70/80 MVA, three phase (vector group YNd-1) transformer was manufactured by Sanbian Sci-Tech Co. Ltd. for 230 kV substation of 65 MW power generation plant established by United Generation & Transmission Company Ltd. At the manufacturing industry, SFRA measurement of the transformer was not taken by the Chinese engineers due to unavailability of SFRA machine set-up. As a result, no primary response from the manufacturing factory was available to regard as ‗Standard Response' and to compare.

This transformer was sent by ship from China to Bangladesh. At the Chittagong port, it was shifted to a smaller ship from the foreign vessel. Finally at Ashuganj port, the transformer was shifted to a truck-lorry to its final destination power plant. At the site, an SFRA reading was taken to detect probable mechanical deformation taken place in the active part or not. The response curves and corresponding CCF tables are shown in figure 6.11, 6.12, 6.13 and table 6.8, 6.9, 6.10.
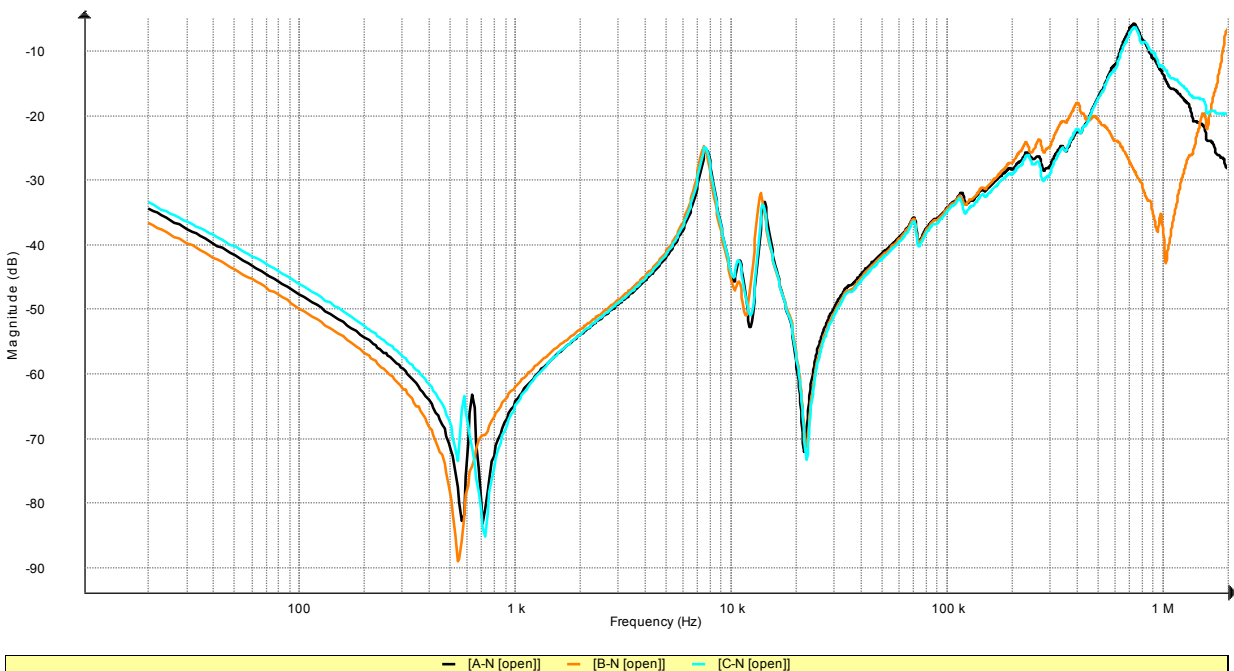
Figure 6.11: HV windings responses keeping the LV windings open (at concern site)

Table 6.8: CCF of HV winding keeping LV open

Frequency Sub-band	CCF results		
	X1-X0, X2-X0	X2-X0, X3-X0	X3-X0, X1-X0
0 – 2 kHz	0.998	0.996	0.998
2 kHz – 20 kHz	0.971	0.970	0.979
20 kHz – 400 kHz	0.952	0.954	0.975
400 kHz – 1 MHz	-0.765	-0.757	0.969
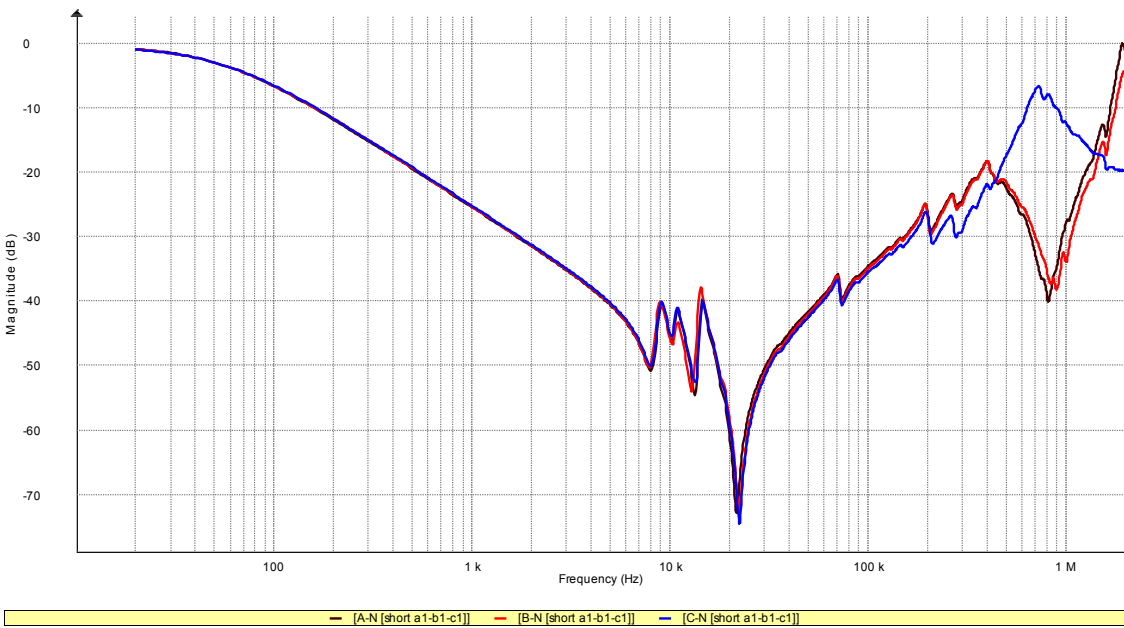
Figure 6.12: HV windings responses keeping the LV windings Shorted (at concern site)

Table 6.9: CCF of HV winding keeping LV short

Frequency Sub-band	CCF results		
	X1-X0, X2-X0	X2-X0, X3-X0	X3-X0, X1-X0
0 – 2 kHz	0.999	0.999	0.999
2 kHz – 20 kHz	0.979	0.983	0.981
20 kHz – 400 kHz	0.982	0.953	0.959
400 kHz – 1 MHz	0.978	-0.627	-0.695
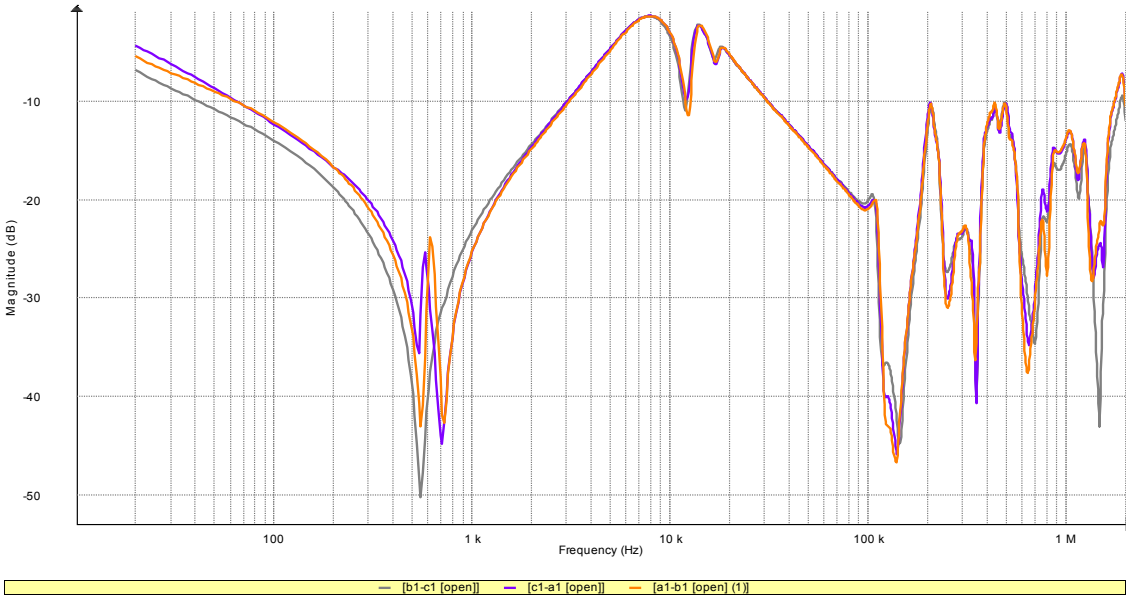
Figure 6.13: LV windings responses keeping the HV windings open (at concern site)

Table 6.10: CCF of LV winding keeping HV open

Frequency Sub-band	CCF results		
	X1-X0, X2-X0	X2-X0, X3-X0	X3-X0, X1-X0
0 – 2 kHz	0.989	0.993	0.991
2 kHz – 20 kHz	0.988	0.990	0.986
20 kHz – 400 kHz	0.972	0.975	0.969
400 kHz – 1 MHz	0.962	0.967	0.981

From the CCF table 6.8 and 6.9, it is clearly visible that, at the highest voltage region (400 kHz ~ 1 MHz), the B-phase response of High Voltage winding showing absurd result with respect to A & C phase response when Low Voltage side is open and the C-phase response of High Voltage winding showing absurd result with respect to A & B phase response when High Voltage side is shorted. So no doubt to tell about that the fault which has taken place in high voltage winding beggars' description and this fault has also been sensed in other electrical tastings. The CCF results for Low Voltage windings are normal. So all the Low Voltage windings are at healthy condition and not severely deformed. This transformer was marked as faulty one and has been sent back to China for repairing.

Chapter 7

Conclusion

7.1   Conclusion

In this thesis, Sweep frequency response analysis method has been applied successfully to a number of three phase and single phase power transformers of different vector groups, to detect mechanical deformation, according with Cross Correlation Co-Efficient (CCF) as interpreting parameter. This method is also applicable for mechanical deformation and damage diagnosis in distribution transformers. The parameter Cross Correlation Co-efficient (CCF) is found to vary significantly and consistently with mechanical displacements taken place in transformers. So it can be considered as one of the most effective indicator to predict the internal physical condition of the active part of a transformer.

The MATLAB code which has been used for point extraction from SFRA curves is developed to extract 150 points from each trace. If the code is modified to extract more points then obviously the result will be more precise. In that case, the processor of the concern computer will face more stress and the calculation time will be a bit more.

This method using CCF is fully efficient for fault detection of Y-connected windings of a transformer. But in case of Delta connected windings, this method will fail to detect a fault in a specific winding. In this thesis, the concern transformer which had faulty Delta connection, had deformations in all three windings of the Delta side. For this reason, the aforementioned lacking of CCF method didn't affect the concern case study.

7.2   Recommendation for Further Research

It is found that Normalization Covariance Factor (NCF) can be a reliable statistical indicator to extract information from comparison method. If X_i and are Y_i are the two series (or trace in the case of SFRA) being compared at each individual frequency _i' and X-bar and Y-bar are the means then the standard variance of these two sequences are calculated as

$$D_x = \frac{1}{N} \sum_{K=0}^{N-1} \left[X(K) - \frac{1}{N} \sum_{K=0}^{N-1} X(K) \right]^2$$

$$D_y = \frac{1}{N} \sum_{K=0}^{N-1} \left[Y(K) - \frac{1}{N} \sum_{K=0}^{N-1} Y(K) \right]^2$$

The formula to calculate the covariance of these two sequences is

$$C_{xy} = \frac{1}{N} \sum_{K=0}^{N-1} \left[X(K) - \frac{1}{N} \sum_{K=0}^{N-1} X(K) \right]^2 \times \left[Y(K) - \frac{1}{N} \sum_{K=0}^{N-1} Y(K) \right]^2$$

The Normalization Covariance Factor (NCF) of these sequences is

$$LR_{xy} = C_{xy} / \sqrt{D_x D_y}$$

The relative factor R_{xy} is formulized in the following way,

$$R_{xy} = \begin{cases} 10 & , \quad 1 - LR_{xy} < 10^{-10} \\ -\log(1 - LR_{xy}) & , \quad others \end{cases}$$

As the calculation formula for Relative Factor R_{xy} of Normalization Covariance is more complicated with respect to Cross Correlation Co-Efficient (CCF) so the MATLAB code which have to be developed for this method will be more completed with respect to the MATLAB code developed for this thesis.

In SFRA analysis negative NCF are not common but they do occur on occasion. Regardless, negative covariance factors are not considered acceptable when trying to look for deviations between traces

References

1. McGrail T., "Transformer Frequency Response Analysis: An Introduction", Feature Article NETA WORLD, Spring 2005.

2. Darveniza M., Hill D. J.T., Le T.T. and Saha T. K., "Investigations into Effective Methods for Assessing the Condition of Insulation in Aged Power transformers", IEEE Trans. Power delivery, Vol 13, pp.1214-1223, 1998.

3. Huellmandel F., Boehm K., Neumann C., Koch N., Loppach K., Krause C., Alff J. J., "Condition Assessment of Aged Transformer Bushing Insulations", Paper A2-104, CIGRE, Paris, France, pp. 1-10. 2006.

4. Nigris M. D. et. al.,"Application of Modern Techniques for the Condition Assessment of Power Transformers", Cigré Session 2004, Paper No.A2-207.

5. Richardson B., "Diagnostics and Condition Monitoring of Power Transformers" IEEE, ABB Power Transformer Research and Development Ltd, 1997.

6. Purnomoadi A. P., Fransisco D., "Modeling and diagnostic transformer condition using Sweep Frequency Response Analysis", Proc. ICPADM 9th International Conference on the Properties and Applications of Dielectric Materials, pp. 1059 – 1063, July 2009. doi: 10.1109/ ICPADM.2009.5252450. (IEEE Transaction)

7. Werelius P., Ohlen M., Adeen L., Brynjebo E., Taby T., "Measurement considerations using SFRA for condition assessment of Power Transformers", Proc. CMD International Conference on Condition Monitoring and Diagnosis, pp. 898-901, April 2008. doi: 10.1109/ CMD.2008.4580428 (IEEE Transaction)

8. Joginadham G., Mangalvedekar H. A., Venkatasami A., "Development of networks for SFRA data using circuit synthesis", Proc. CMD International Conference on Condition Monitoring and Diagnosis, pp. 1350-1353, April 2008. doi: 10.1109/CMD.2008.4580519 (IEEE Transaction)

9. Patil S., Venkatasami A., "Realization of transformer winding network from sweep frequency response data" Proc. CMD International Conference on Condition Monitoring and Diagnosis, pp. 505-508, April 2008. doi: 10.1109/CMD.2008.4580336 (IEEE Transaction)

10. Al-Ammar E., Karady G., Hevia O. P., "Improved Technique for Fault Detection Sensitivity in Transformer Maintenance Test" Proc. Power Engineering Society General Meeting, pp. 505-508, June 2007. doi: 10.1109/PES.2007.385614 (IEEE Transaction).

11. S. Ryder, "Diagnosing Transformer faults using frequency response analysis: Results from fault simulations". IEEE/PES Summer Meeting, Chicago, pp. 399-404, 2002.

12. Islam S. M., "Detection of Shorted Turns and Winding Movements in Large Power Transformers Using Frequency Response Analysis", IEEE Power Society, Winter Meeting, Singapore, vol.3, pp. 2233-2238, 2000.

13. Lapworth J. A. and Noonan T. J., "Mechanical condition assessment of power transformers using frequency response analysis" Proceedings of International Client Conference, Boston, MA, USA, 1995

14. Coffeen L., Britton J., Rickmann J., ─A New Technique to Detect Winding Displacements in Power Transformers Using Frequency Response Analysis", IEEE PowerTech Conference, pp. 23-26, Bologna, Italy, June 2003.

15. Moodley L., Klerk B. D., ─Sweep Frequency Response Analysis as A Diagnostic tool to Detect Transformer Mechanical Integrity", eThekwini Electricity pp.1-9, 1978

16. Tenbohlen S., Ryder S. A., ─Making Frequency Response Analysis Measurements: A Comparison of the Swept Frequency and Low Voltage Impulse Methods", XIIIth International Symposium on High Voltage Engineering, Smit (ed), © 2003 Millpress, Rotterdam, ISBN 90-77017-79-8, Netherlands 2003

17. M. Wang, A. J. Vandermaar, K. D. Srivastava, ─Transformer Winding Movement Monitoring in Service—Key Factors Affecting FRA Measurements", IEEE Electrical Insulation Magazine, Vol. 20, No. 5, pp 5-12, 2004.

18. Tenbohlen S. and Ryder S. A., ─Making Frequency Response Analysis Measurements, a Comparison of the Swept Frequency and LV Impulse Methods". 13th International Symposium on HV Engineering, Netherlands, 2003.

19. Bak-Jensen J., Jensen B. B. and Mikkelsen S. D., ─Detection of Faults and Aging Phenomena in Transformers by Transfer Functions", IEEE Transactions on Power Delivery, vol.10, no.1, January 1999.

20. Zhijian J., Jingtao L., Zishu Z., ─Diagnosis of Transformer Winding Deformation on the Basis of Artificial Neural Network", Proceedings of The 6th International Conference on Properties and Applications of Dielectric Materials, Xi'an Jiaotong University, Xi'an, China, May 21-26, 2000.

21. Saha T. K., Prasad A., Yao, Z. T., ─Voltage Response Measurements for the Diagnosis of Insulation Condition in Power Transformer", International Symposium on High Voltage Engineering, August 19-25, 2001, Paper 6-8, Bangalore, India.

22. Dorf R.C. and Bishop R.H. (2005). ─Modern Control Systems" 10th ed. Dorling Kindersley, New Delhi, 869p.

23. Cogger N.D., Webb R.V., ─Frequency Response Analysis", Solartron Analytical, Technical Report 10, 1997.

24. Saha, T.K., Purkait, P., ─An Attempt to Correlate Time & Frequency Domain Polarisation Measurements for the Insulation Diagnosis of Power Transformer" , Proceedings of the IEEE Power Engineering Society General Meeting, Denver, Colorado, USA , June 6-10 2004.

25. Ryder S., ─Methods for comparing frequency response analysis measurements". IEEE, Int. Symp. Electrical Insulation, pp.187-190, Boston, 2002

APPENDIX – A

Table A.1   Nameplate data of the 40/50 MVA, 132/11 kV transformer

REF. NO.	DOC. NO.	CHANGE DETAILS		ALL DIMENSIONS ARE IN mm	DATE	PRD.	APPD.
				UNSPECIFIED TOLERANCE ± 1%			

40/50 MVA POWER TRANSFORMER

ENERGYPAC®
AN ISO 9001&14001 CERTIFIED COMPANY

TYPE OF COOLING	ONAN/ONAF	STANDARD	BS–171/IEC–76		
RATED MVA	40/50	FREQUENCY	HZ	50	
RATED KV — HV	132			LI 650 AC 275	
RATED KV — LV	11	INSULATION LEVEL	HV / HVN / LV	KV LI 95 AC 38 / LI 75 AC 28	
RATED LINE CURRENT (Amp.) — HV	174.95/218.69	CORE & COIL		35000	
RATED LINE CURRENT (Amp.) — LV	2099.45/2624.31	TANK & FITTINGS		21500	
VECTOR GROUP	YNd1	MASS OF OIL	KG	24500	
NO OF PHASES	3	TOTAL MASS		81000	
% IMPEDANCE		TRANSPORT MASS		59000	
TEMP RISE °C — TOP OIL	50	VOLUME OF OIL	L	28100	
TEMP RISE °C — AVG. WDG	55				
YEAR OF MFG.		MAKER'S REF. NO.			
DIAGRAM DRG. NO.	PP40/D36–40004	MAKER'S SERIAL NO.			
CUSTOMER'S REF. NO.					

TAP POSITION	CHANGE OVER SELECTOR	LEADS JOINED	HV LINE VOLTS	HV AMPS.	LV LINE VOLTS	LV AMPS.
1		A–1	145200	159.04/198.81		
2		A–2	143550	160.87/201.10		
3		A–3	141900	162.74/203.44		
4		A–4	140250	164.66/205.83		
5		A–5	138600	166.62/208.28		
6		A–6	136950	168.63/210.79		
7	O +	A–7	135300	170.68/213.36		
8		A–8	133650	172.79/215.99		
9		A–9	132000	174.95/218.69	11000	2099.45/2624.31
10		A–10	130350	177.17/221.46		
11		A–11	128700	179.44/224.30		
12		A–12	127050	181.77/227.22		
13a		A–13	125400	184.16/230.21		
13b		A–K	125400	184.16/230.21		
13c		A–1	125400	184.16/230.21		
14		A–2	123750	186.61/233.27		
15		A–3	122100	189.14/236.43		
16		A–4	120450	191.73/239.67		
17	O –	A–5	118800	194.39/242.99		
18		A–6	117150	197.13/246.42		
19		A–7	115500	199.95/249.94		
20		A–8	113850	202.85/253.56		
21		A–9	112200	205.83/257.29		
22		A–10	110550	208.90/261.13		
23		A–11	108900	212.07/265.09		
24		A–12	107250	215.33/269.16		
25		A–13	105600	218.69/273.37		

CURRENT TRANSFORMER

	RATIO	ACC CLASS	BURDEN (VA)	QTY.	PURPOSE
HVCT	300/1A	5P20	30	3	DIFF. PROTECTION
HVNCT	300/1–1A	5P20	30	1	REF. PROTECTION
LVCT	3600/1A	5P20	30	3	DIFF. PROTECTION
WTI	2627/5A	0.5	20	1	WINDING TEMPERATURE

ENERGYPAC ENGINEERING LTD.
MADE IN BANGLADESH

CONTRACTOR: ENERGYPAC ENGINEERING LTD.	
CUSTOMER: PRECISION ENERGY LTD.	
TITLE: RATING & DIAGRAM PLATE FOR 40/50 MVA, 132/11 KV, 3 Ph, 50 Hz, YNd1 POWER TRANSFORMER.	DRAWING No. TR3-A4-PP-40/50M-40004

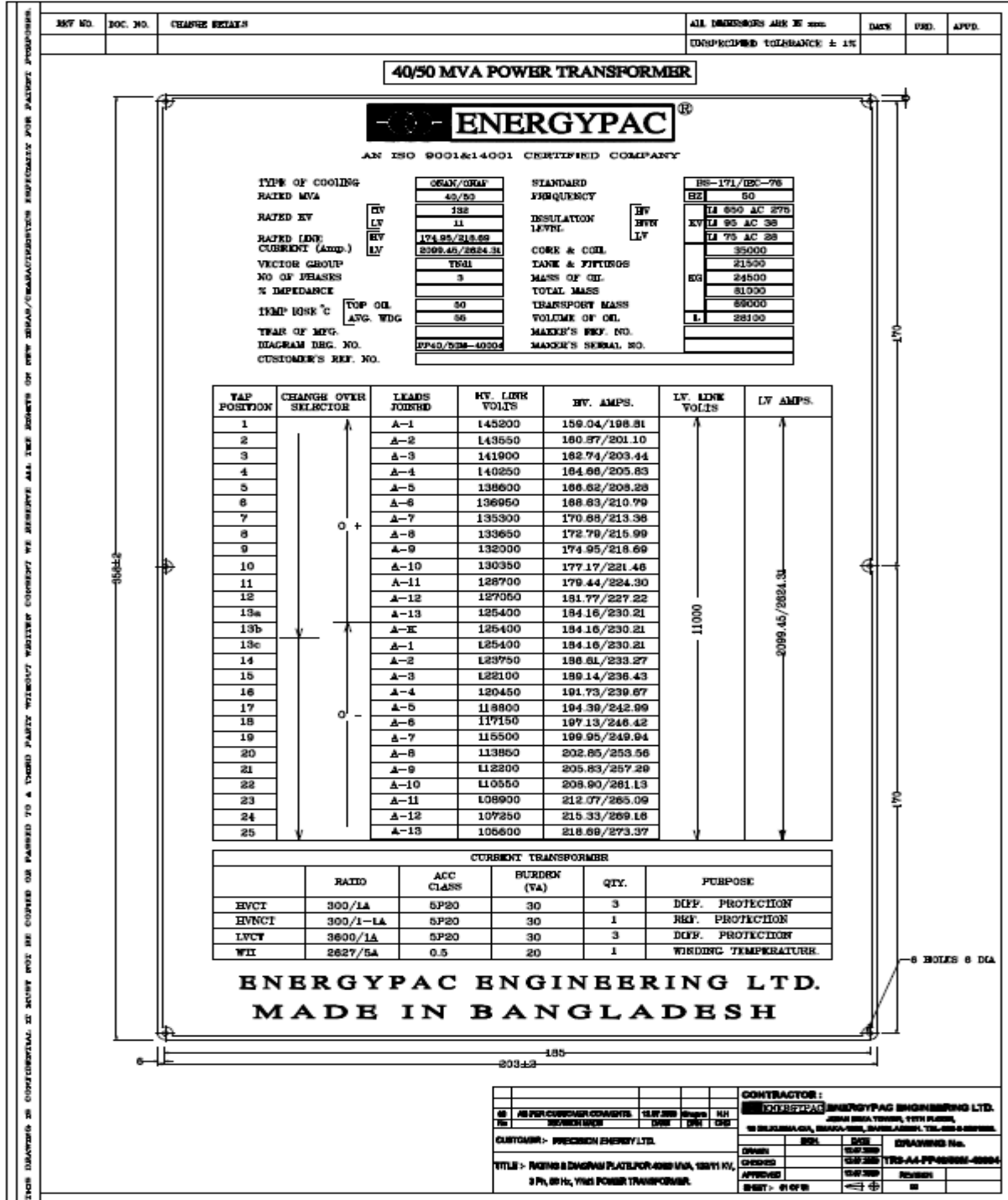# Table A.2 Connection diagram of the 40/50 MVA, 132/11 kV transformer

Table A.3   Nameplate data of the 20/25 MVA, 132/11 kV transformer

REV NO.	DOC. NO.	CHANGE DETAILS		ALL DIMENSIONS ARE IN mm	DATE	PRD.	APPD.
				UNSPECIFIED TOLERANCE ± 1%			

ENERGYPAC ®
AN ISO 9001 & 14001 CERTIFIED COMPANY

SINGLE PHASE STEP UP GENERATING TRANSFORMER.

TYPE OF COOLING	ONAN/ONAF	
RATED KVA	20000/25000	
PHASE	1	
RATED VOLTAGE KV	HV 132/√3	
	LV 11	
RATED LINE CURRENT (Amp.)	HV 262.43/328.04	
	LV 1818.18/2272.73	
POLARITY	SUBTRACTIVE	
% IMPEDANCE		
TEMP RISE °C	TOP OIL 55	
	AVG.WDG 60	
YEAR OF MFG.		
DIAGRAM DRG. NO.	TR1-A3-PP25MS-04	

STANDARD	IEC-60076	
FREQUENCY HZ	50	
INSULATION LEVEL	HV LI 650 AC 275	
	HVN KV LI 95 AC 38	
	LV LI 75 AC 28	
CORE & COIL	20300	
TANK & FITTINGS	11000	
MASS OF OIL KG	12700	
TOTAL MASS	44000	
TRANSPORT MASS	34000	
VOLUME OF OIL L	14600	
MAKER'S REF. NO.		
MAKER'S SERIAL NO.		
CUSTOMER'S REF. NO.		

RATING PLATE FOR 'A' PHASE.

aS4
aS3
aS2
aS1

a1   a2

N   A

AS2
AS1
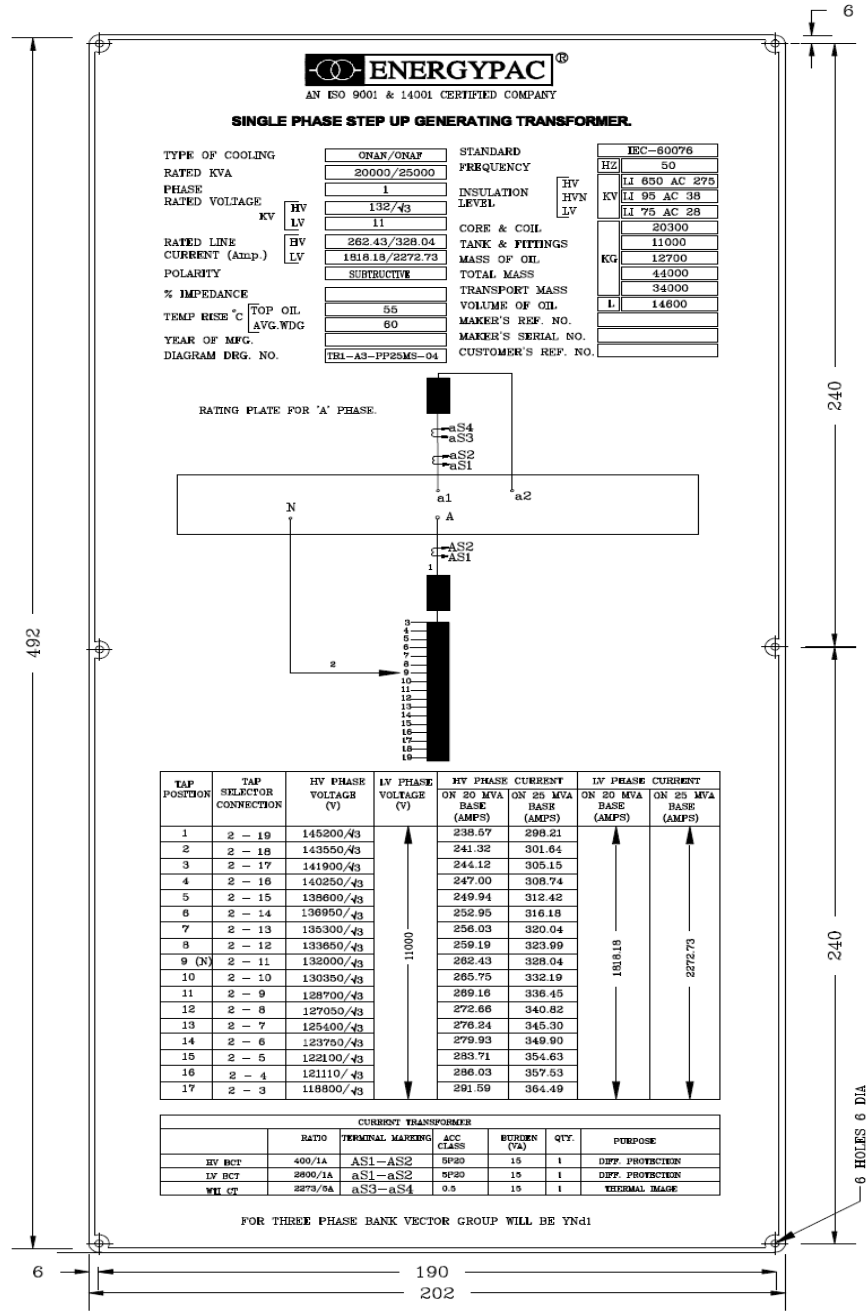
TAP POSITION	TAP SELECTOR CONNECTION	HV PHASE VOLTAGE (V)	LV PHASE VOLTAGE (V)	HV PHASE CURRENT ON 20 MVA BASE (AMPS)	HV PHASE CURRENT ON 25 MVA BASE (AMPS)	LV PHASE CURRENT ON 20 MVA BASE (AMPS)	LV PHASE CURRENT ON 25 MVA BASE (AMPS)
1	2 − 19	145200/√3		238.57	298.21		
2	2 − 18	143550/√3		241.32	301.64		
3	2 − 17	141900/√3		244.12	305.15		
4	2 − 16	140250/√3		247.00	308.74		
5	2 − 15	138600/√3		249.94	312.42		
6	2 − 14	136950/√3		252.95	316.18		
7	2 − 13	135300/√3		256.03	320.04		
8	2 − 12	133650/√3		259.19	323.99		
9 (N)	2 − 11	132000/√3	11000	262.43	328.04	1818.18	2272.73
10	2 − 10	130350/√3		265.75	332.19		
11	2 − 9	128700/√3		269.16	336.45		
12	2 − 8	127050/√3		272.66	340.82		
13	2 − 7	125400/√3		276.24	345.30		
14	2 − 6	123750/√3		279.93	349.90		
15	2 − 5	122100/√3		283.71	354.63		
16	2 − 4	121110/√3		286.03	357.53		
17	2 − 3	118800/√3		291.59	364.49		

CURRENT TRANSFORMER						
	RATIO	TERMINAL MARKING	ACC CLASS	BURDEN (VA)	QTY.	PURPOSE
HV BCT	400/1A	AS1−AS2	5P20	15	1	DIFF. PROTECTION
LV BCT	2600/1A	aS1−aS2	5P20	15	1	DIFF. PROTECTION
WTI CT	2273/5A	aS3−aS4	0.5	15	1	THERMAL IMAGE

FOR THREE PHASE BANK VECTOR GROUP WILL BE YNd1

6 HOLES 6 DIA

CONTRACTOR :
ENERGYPAC ENGINEERING LTD.
JIBAN BIMA TOWER, 11TH FLOOR,
10 DILKUSHA C/A, DHAKA-1000, BANGLADESH. TEL-880-2-9661883.

00	AS PER CUSTOMER COMMENTS.	03.11.2010	KABIR	N.H
No	REVISION MADE	DATE	DRN	CHD

CUSTOMER :-

	SIGN.	DATE	DRAWING No.
DRAWN		02.11.2010	TR1-A3-PP25MS-04
CHECKED		02.11.2010	
APPROVED		02.11.2010	REVISION SCALE
SHEET :- 01 OF 01			00 NTS

TITLE :- RATING & DIAGRAM PLATE FOR 20/25 MVA,
132/√3/11 kV, 1 Ph, 50 Hz, TRANSFORMER.

Table A.4   Nameplate data of the 10/14 MVA, 33/11 kV transformer

REV NO.	DOC. NO.	CHANGE DETAILS		ALL DIMENSIONS ARE IN mm	DATE	PRD.	APPD.
				UNSPECIFIED TOLERANCE ± 1%			

10/14 MVA POWER TRANSFORMER

ENERGYPAC®
ISO 9001:14001 CERTIFIED COMPANY

TYPE OF COOLING		ONAN/ONAF	STANDARD		BS-171/76
RATED MVA		10/14	FREQUENCY	HZ	50
RATED KV	HV	33	INSULATION LEVEL	HV	LI 170 AC 70
	LV	11		LV	LI 75 AC 28
RATED LINE CURRENT (Amp.)	HV	174.9/244.9		LVN	LI 75 AC 28
	LV	524.9/734.8		KV	
VECTOR GROUP		Dyn 11	CORE & COIL		12000
NO OF PHASES		3	TANK & FITTINGS		8400
% IMPEDANCE ON 14 MVA			MASS OF OIL	KG	6180
TEMP RISE °C	TOP OIL	60	TOTAL MASS		26580
	AVG. WDG	65	TRANSPORT MASS		23100
YEAR OF MFG.			VOLUME OF OIL	L	7100
DIAGRAM DRG. NO.		P14M-14004	MAKER'S REF. NO.		
CUSTOMER'S REF. NO.			MAKER'S SERIAL NO.		

Dyn 11

TAP POSITION	CHANGE OVER SELECTOR	LEADS JOINED	HV. LINE VOLTS	HV. AMPS.	LV. LINE VOLTS	LV AMPS.
1		A - 1	36300	159.05/222.7		
2		A - 2	35887.5	160.9/225.2		
3		A - 3	35475	162.8/227.9		
4		A - 4	35062.5	164.7/230.6		
5	0 +	A - 5	34650	166.6/233.2		
6		A - 6	34237.5	168.6/236.0		
7		A - 7	33825	170.7/239.0		
8		A - 8	33412.5	172.8/241.9		
9a		A - 9	33000	174.9/244.9	11000	524.9/734.8
9b		A - K	33000	174.9/244.9		
9c		A - 1	33000	174.9/244.9		
10		A - 2	32587.5	177.2/248.0		
11	0 -	A - 3	32175	179.4/251.1		
12		A - 4	31762.5	181.8/254.5		
13		A - 5	31350	184.2/257.9		
14		A - 6	30937.5	186.6/261.2		
15		A - 7	30525	189.1/264.7		
16		A - 8	30112.5	191.7/268.4		
17		A - 9	29700	194.4/272.2		

CURRENT TRANSFORMER

	RATIO	ACC CLASS	BURDEN (VA)	QTY.	PURPOSE
HVCT	300/1	5P10	15	3	DIFF. PROTECTION
LVCT	900/1	5P10	15	3	DIFF. PROTECTION
LVNCT	900/1	5P10	15	1	REF. PROTECTION
WTI	735/5	5P10	15	1	WINDING TEMPERATURE.
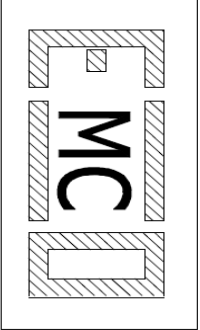
ENERGYPAC ENGINEERING LTD.
MADE IN BANGLADESH

00	AS PER CUSTOMER COMMENTS.	27.06.2011 Shopna Anjan	CONTRACTOR : ENERGYPAC ENGINEERING LTD.
No	REVISION MADE	DATE DRN CHD	JIBAN BIMA TOWER, 11TH FLOOR, 10 DILKUSHA C/A, DHAKA-1000, BANGLADESH. TEL-880-2-9551863.

CUSTOMER :

TITLE : RATING & DIAGRAM PLATE OF 10/14 MVA, 33/11 kV, 3 Ph, 50 Hz ONAN/ONAF TRANSFORMER.

	SIGN.	DATE	DRAWING No.
DRAWN		27.06.2011	TR3-A3-P14M-14004
CHECKED		27.06.2011	
APPROVED		27.06.2011	REVISION: 00 / SCALE: NTS
SHEET :- 01 OF 01			

Table A.5 Nameplate data of the 25/41.67 MVA, 132/33 kV transformer

EMCO TRANSFORMERS LTD.

MC (logo)

POWER TRANSFORMER

MAHARASTHRA

SPECIFICATION REF NO.		IEC-60076	
TYPE OF COOLING		ONAN	ONAF
RATED POWER	HV KVA	25000	41670
	LV KVA	25000	41670
RATED VOLTAGE (AT-NO LOAD)	HV KV	132	132
	LV KV	33	33
RATED LINE CURRENT	HV A	109.35	182.26
	LV A	437.39	729.04

PHASES		THREE
FREQUENCY HZ		50
VECTOR GROUP		Dyn 1
INSULATION LEVEL	HV KV	LI650/AC275
	LV/LVn KV	LI170/AC70
CORE & WINDING MASS KG		32000
MASS OF OIL KG		21135
TANK & FITTINGS MASS KG		25365
TOTAL MASS KG		78500
TRANSPORT MASS KG		43000
VOLUME OF OIL LIT.		28500
DIAGRAM DRG. NO.		2/11/105/R.
MAKER'S SERIAL NO.		HT 1402/11798
YEAR OF MANUFACTURE		

GUARANTED MAX TEMPERATURE RISE	TOP OIL °C	55
	WINDING °C	65
REFERENCE AMBIENT TEMP °C		40
IMPEDANCE VOLTAGE HV. LV	TAP NO. 1	10.93
	TAP NO. 9 %	11.57
(ON 41.67 MVA BASE)	TAP NO. 17%	12.37

CUSTOMER'S REFERENCE : CONTRACT-NO. PUR-363/95, DATED: 04/08/97

CUSTOMER : BANGLADESH POWER DEVELOPMENT BOARD